Miscellaneous Paper SL-93-8
July 1993

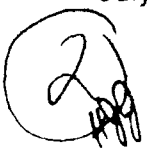

US Army Corps of Engineers
Waterways Experiment Station

Simulation of Gage-Mount Responses in Airblast Tests

by C. Wayne Mastin
Mississippi State University

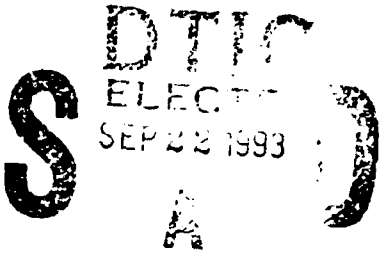

Approved For Public Release; Distribution Is Unlimited

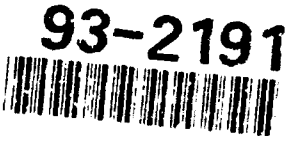

Prepared for Defense Nuclear Agency

The contents of this report are not to be used for advertising, publication, or promotional purposes. Citation of trade names does not constitute an official endorsement or approval of the use of such commercial products.

PRINTED ON RECYCLED PAPER

Miscellaneous Paper SL-93-8
July 1993

Simulation of Gage-Mount Responses in Airblast Tests

by C. Wayne Mastin

Department of Mathematics and Statistics
Mississippi State University
Mississippi State, MS 39762

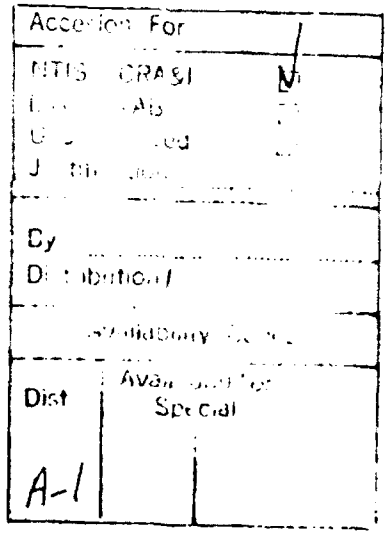

Final report

Approved for public release; distribution is unlimited

Prepared for Defense Nuclear Agency
Kirtland Air Force Base, NM 87117-5000

Under Contract No. DACA39-90-M-3694

Monitored by Structures Laboratory
U.S. Army Engineer Waterways Experiment Station
3909 Halls Ferry Road, Vicksburg, MS 39180-6199

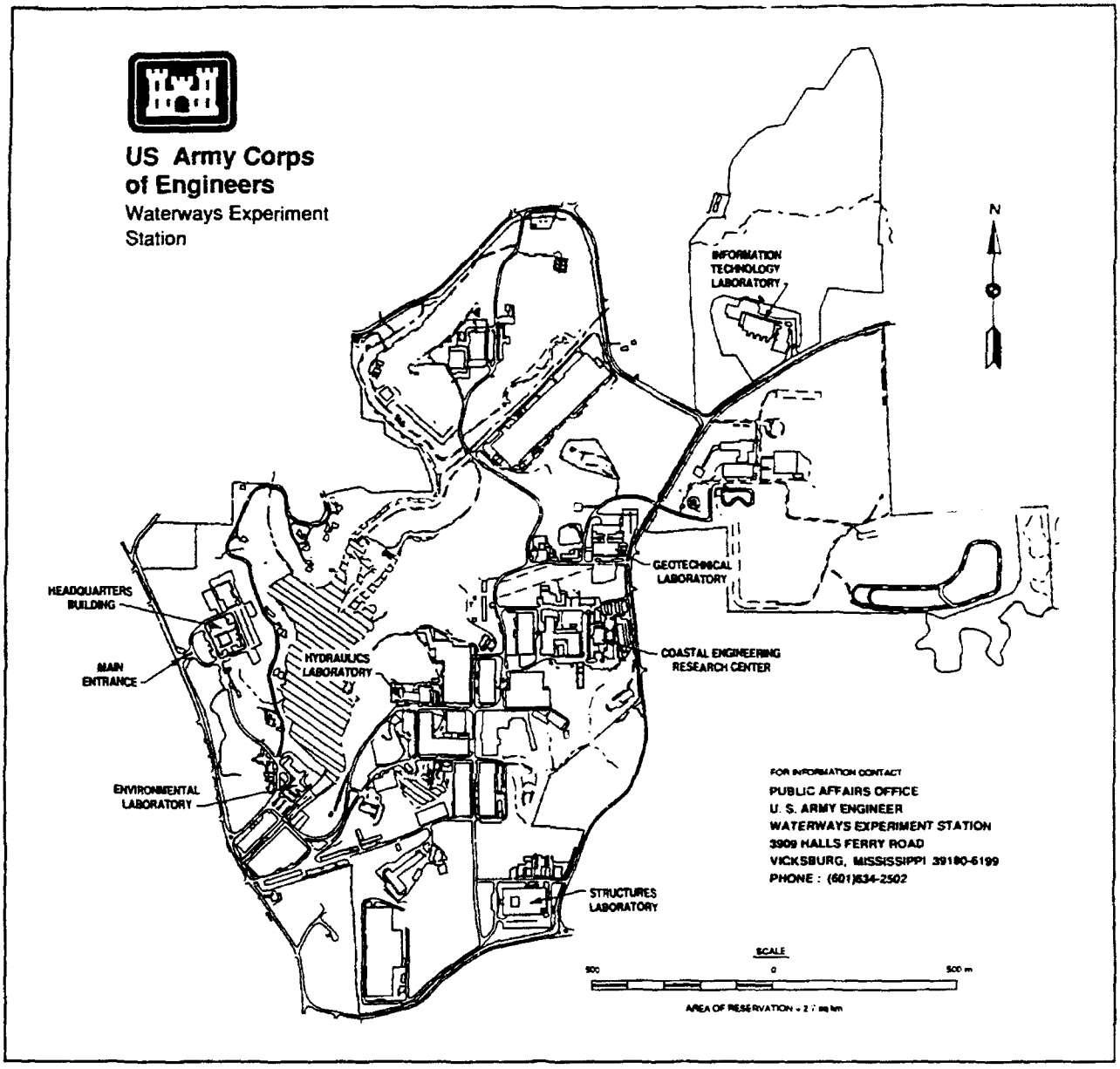

Waterways Experiment Station Cataloging-In-Publication Data

Mastin, C. Wayne.
Simulation of gage-mount response in airblast tests / by C. Wayne Mastin ; prepared for Defense Nuclear Agency ; monitored by Structures Laboratory, U.S. Army Engineer Waterways Experiment Station.
45 p. : ill. ; 28 cm. — (Miscellaneous paper ; SL-93-8)
Includes bibliographical references.
1. Blast effect — Simulation methods. 2. Aerodynamic load — Data processing. 3. HULL (Computer program) 4. Blast effect — Measurement — Instruments. I. United States. Defense Nuclear Agency. II. U.S. Army Engineer Waterways Experiment Station. III. Title. IV. Series: Miscellaneous paper (U.S. Army Engineer Waterways Experiment Station) ; SL-93-8.
TA7 W34m no.SL-93-8

1 PREFACE

This study was conducted for Headquarters, U. S. Army Corps of Engineers, under Contract No. DACA39-90-M-3694. The work was performed under the sponsorship of the Field Command, Defense Nuclear Agency (MIPR HD 1102-0-H24A03). The research was accomplished by Dr. C. Wayne Mastin, Mississippi State University, at the Explosion Effects Division (EED), Structures Laboratory (SL), U. S. Army Engineer Waterways Experiment Station (WES), under the technical supervision of Mr. Howard G. White, EED.

This report was prepared under the general supervision of Mr. Bryant Mather, Director, SL, and Mr. L. K. Davis, Chief, EED. The work was performed by Dr. Mastin in collaboration with Messrs. Charles R. Welch, White, and Byron J. Armstrong, EED.

At the time of publication of this report, Director of WES was Dr. Robert W. Whalin. Commander was COL Leonard G. Hassell, EN.

Contents

2 LIST OF FIGURES

24. Pressure time history at 10.0-cm ground range, with gage mount included.

25. Pressure time history at 10.0-cm ground range, with no gage mount.

26. Pressure time history at 5.0 cm below ground zero, near center of steel cylinder.

27. Pressure time history at 5.0 cm below ground zero, with no gage mount.

28. Pressure time history at 15.0 cm below ground zero, in concrete housing below steel cylinder.

29. Pressure time history at 15.0 cm below ground zero, with no gage mount.

30. Comparison of HULL-calculated pressure time history at ground zero with results from a SHARC calculation. The HULL solution has been shifted to match the experimental time-of-arrival.

31. Comparison of HULL-calculated pressure time history at ground zero with results from the Mineral Find II, gage no. 47. The HULL solution has been shifted to match the experimental time-of-arrival.

32. Comparison of HULL-calculated pressure time history at ground zero with results from the Mineral Find II, gage no. 48. The HULL solution has been shifted to match the experimental time-of-arrival.

33. Pressure impulse time history at ground zero from HULL and SHARC calculations compared with results of the Mineral Find II experiment. The HULL solution has been shifted to match the experimental time-of-arrival.

THE SIMULATION OF GAGE MOUNT RESPONSES IN AIRBLAST TESTS

3 INTRODUCTION

A set of airblast experiments called Mineral Find I, II, and III were completed on 24 April 1990. The data collected revealed high frequency anomalies which may be due to either the gage mount or the explosive. In order to gain a better understanding of this phenomenon, the HULL code was used to simulate one of these events, Mineral Find II (MFII). The code was run with and without the gage mount to assess the effect of the mount on the solution. The computed solution with the gage mount is compared with the experimental results and with another numerical solution. The numerical solution computed from the HULL code exhibits most features of the experimental results. The main deficiency in the numerical solution is in the prediction of the airblast arrival time. All computations in this report were done on the Cray YMP computer at WES.

4 COMPUTATIONAL PROCEDURES

The materials and geometry of the MFII test were modeled using the material properties and geometry options in the HULL program. The following materials were used for this problem.

AIR - with the Doan-Nickle equation-of-state

HMXBRN - burned HMX explosive

SAND - dry Eglin AFB sand (for soil model)

CONCRT - concrete

SSTEEL - stainless steel

For the MFII test, a spherical charge was located 304.8 cm above the ground. A gage mounted on a cylindrical steel and concrete platform was located at ground zero (directly below the center of the charge). A sketch of the initial setup for the test is given in Figure 1. The gage is located at the origin of the coordinate system. The gage mount is sketched in Figure 2. The radius of the spherical charge of HMX explosive was assumed to be 38 cm. The charge consisted of approximately 453 kg of explosive. Due to symmetry, this problem can be solved as a two-dimensional axisymmetric problem with a vertical axis of symmetry passing through the center of the charge. A computational grid must be selected which will both model the initial

stage of the explosion and also resolve the effects of the explosion on the gage housing. After several preliminary computations (including attempts to use an adaptive grid scheme which was developed last year), the 100 x 400 grid illustrated in Figure 3 was selected. The vertical grid lines are clustered near the axis so that there will be a sufficient number of grid cells along the face of the gage. A close-up view of the grid near the gage mount is plotted in Figure 4. This same grid was used for both computations; i.e., with and without the gage mount.

5 COMPUTATIONAL RESULTS

The plotting capabilities of the HULL package were used to examine and compare the numerical solutions. Since the primary objective was to examine the effect of the gage mount on the numerical solution, the first plots are at a time when the blast front is close to the gage. The nature of the solution before the blast front reaches the gage mount is indicated in Figures 5 through 8. As the blast front nears the gage mount, no oscillations or ringing in the solution are evident. Only the solution with the gage mount is included, since the solution without the mount is almost identical. However, after the blast front hits the mount, there is a distinct difference in the two solutions. This is evident in the contour plots and pressure histograms along the axis of symmetry, which are plotted in Figures 9 through 12. Ringing of the steel casing is indicated in the pressure histogram in Figure 10. Since the wave length is the same as the grid spacing, this could very well be a numerical problem rather than an actual physical phenomena. Without the gage mount, the pressure develops a bimodal form, as seen in Figure 12. The peaks represent a strong shock transmitted through the soil and a weaker shock being reflected from the surface of the soil. Figures 13 through 16 further indicate that the same features of the two solutions persist as the two fronts move in opposite directions. The instabilities in the solution with the gage mount are still present.

Further comparisons of the two solutions can be made from several station plots which give the time histories at selected points. The first station plot is at ground zero, which is also at the center of the top of the gage mount. The effect of the steel cylinder is indicated by the higher pressures in Figure 17 when compared with Figure 18. In both cases, the oscillations in the solution are due to the presence of the surface. At 100 cm above ground zero, the pressure plot, given in Figure 19, is smooth with no oscillations. At 200 cm above ground zero, there is a sharp blast front followed by a broader rise in pressure which slowly dissipates, as indicated in Figure 20. Figure 21 indicates the solution at the edge of the explosive charge. Only one set of figures is included at the stations above ground zero, since the solutions with and without the gage mount were almost identical. The fifth station was located at ground level and 3.75 cm from ground zero. In the problem with the gage mount, this was at a point on top of the concrete housing. Surprisingly, there is very little difference in the two time histories plotted in Figures 22 and 23. At station six, which

is on the surface of the soil in both cases, the two solutions are very similar, as can be seen by comparing Figures 24 and 25. As is apparent in the contour plots and histograms, the real difference in the two solutions is in the steel cylinder. The station plot at a point near the center of the steel casing is given in Figure 26. The high frequency oscillations in the pressure record are clearly evident. As with the spatial oscillations of the casing mentioned previously, this is probably a numerical problem. When the gage mount is not present, these oscillations do not appear in the station plot. That case appears in Figure 27. In an attempt to follow the solution as the shock wave passes through the gage mount, a station was placed at a point in the concrete housing below the steel cylinder. At that point, the solution with the gage mount has completely deteriorated, as indicated in Figure 28. However, even without the housing, some signs of instability in the solution can be seen. The latter case is plotted in Figure 29. This again is a numerical artifact of the shock wave passing into the coarsely gridded region near the bottom of the computational field, compounded by reflections off of the lower boundary.

The numerical results are qualitatively what would be expected, and match the general features of the experimental findings. However, there is still considerable discrepancy between the numerical and experimental data. A comparison of the pressure time histories is contained in Figures 30 through 32. The HULL code predicted a much later time-of-arrival than the experimental data. In all of the comparisons, the HULL pressure graph has been shifted by .15 ms, to match the arrival time of the experimental data. The two curves plotted in Figure 30 are from computed results. One is from the HULL calculations of this report (a rescaling of Figure 17) and the other is from Reference [1]. The latter solution was computed using a one-dimensional method to simulate the blast until the blast front reached the surface at which time the solution was continued using the SHARC hydrodynamics code. The curves plotted in Figures 31 and 32 are comparisons of the HULL calculations with the the MFII experimental data, taken from gages near ground zero. The wave form from the HULL calculations is similar to the other results and the computed pressures are within the uncertainty interval of the experimental data. In particular, the frequencies reported in the experimental data also appear in the computations using the HULL code. Figure 33 contains a comparison of the corresponding impulse values. The larger impulse values in the HULL computations are due to the dissipation of the wave front. This does not occur with the SHARC calculation since it uses a less dissipative numerical algorithm and the computations were started with a high-resolution one-dimensional solver.

Both the solution with and without the gage mount were computed using the default stability factor of STABF = 0.75. However, due to the higher sound speed in steel, the solution with the gage mount took over twice as much computer time. Table 1 lists the computer resources for computing each solution from t = 0.0 to t = 1.2 msec. The time step was essentially constant over the entire computed time interval, so the time needed to compute the solution over any other time interval would be proportional to the values in the table.

Problem	Prob. No.	Time Step	No. of Cycles	CPU Time
With Gage Mount	100	6.13E-7 sec.	1970	2 hr. 7 min.
No Gage Mount	101	1.38E-6 sec.	845	50 min.

Table 1: Computational Resources at t = 1.2 msec.

6 CONCLUSIONS

The computations described in this report verify the fact that the HULL code can be used to model explosive events such as MFII. There is still a need for improvement in the accuracy of the computed results. Although some improvement could be achieved by simply increasing the number of grid points, preliminary computations on a coarse 50×100 grid gave results which were fairly close to the calculations reported here. Therefore, attempting to match the experimental data by simply increasing the number of grid points would soon lead to a problem that would be too large for even the Cray computer. There are other options which could lead to improved results, but these would involve major modifications of the code. For example, the grid points could be used more efficiently by allowing for local grid refinement in regions where there are large solution gradients. A second alternative would be to replace the finite difference algorithm in HULL with a nondissipative algorithm which can more accurately simulate airblast phenomena. Both local grid refinement and the use of nondissipative upwind difference schemes have proven very successful in the solution of difficult problems in aerodynamics, such as the computation of hypersonic flow.

7 REFERENCE

1. Ken Schneider, "1000 lb. HOB Calculations - Data Package", Report No. SSS-DTR-90-11892, S-CUBED Division, Maxwell Laboratories, Albuquerque, New Mexico, September 1990.

8 FIGURES

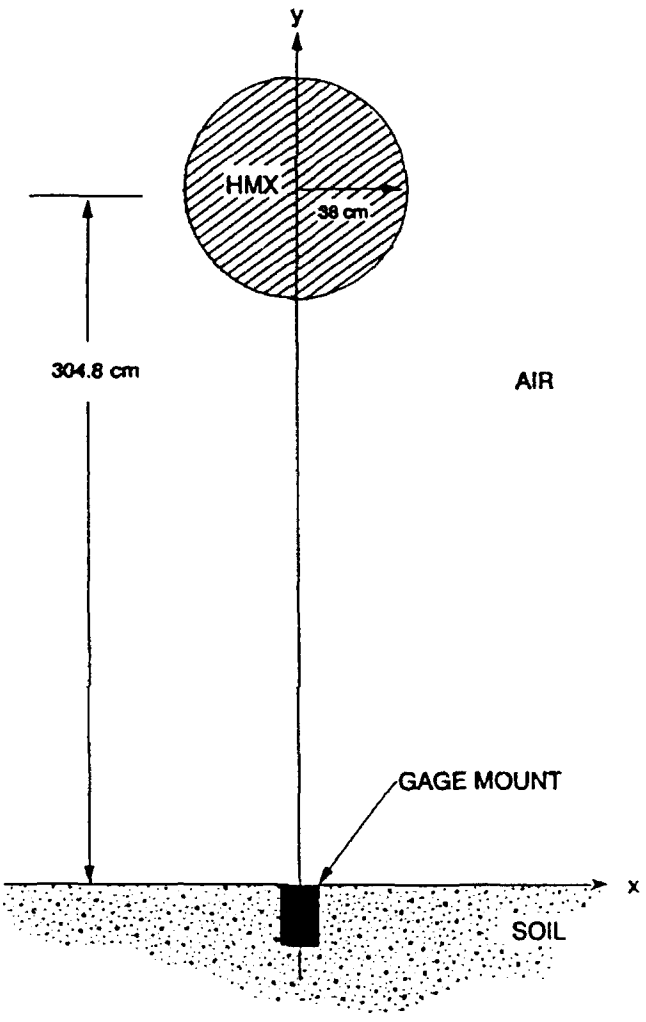

Figure 1. Mineral Find II test configuration.

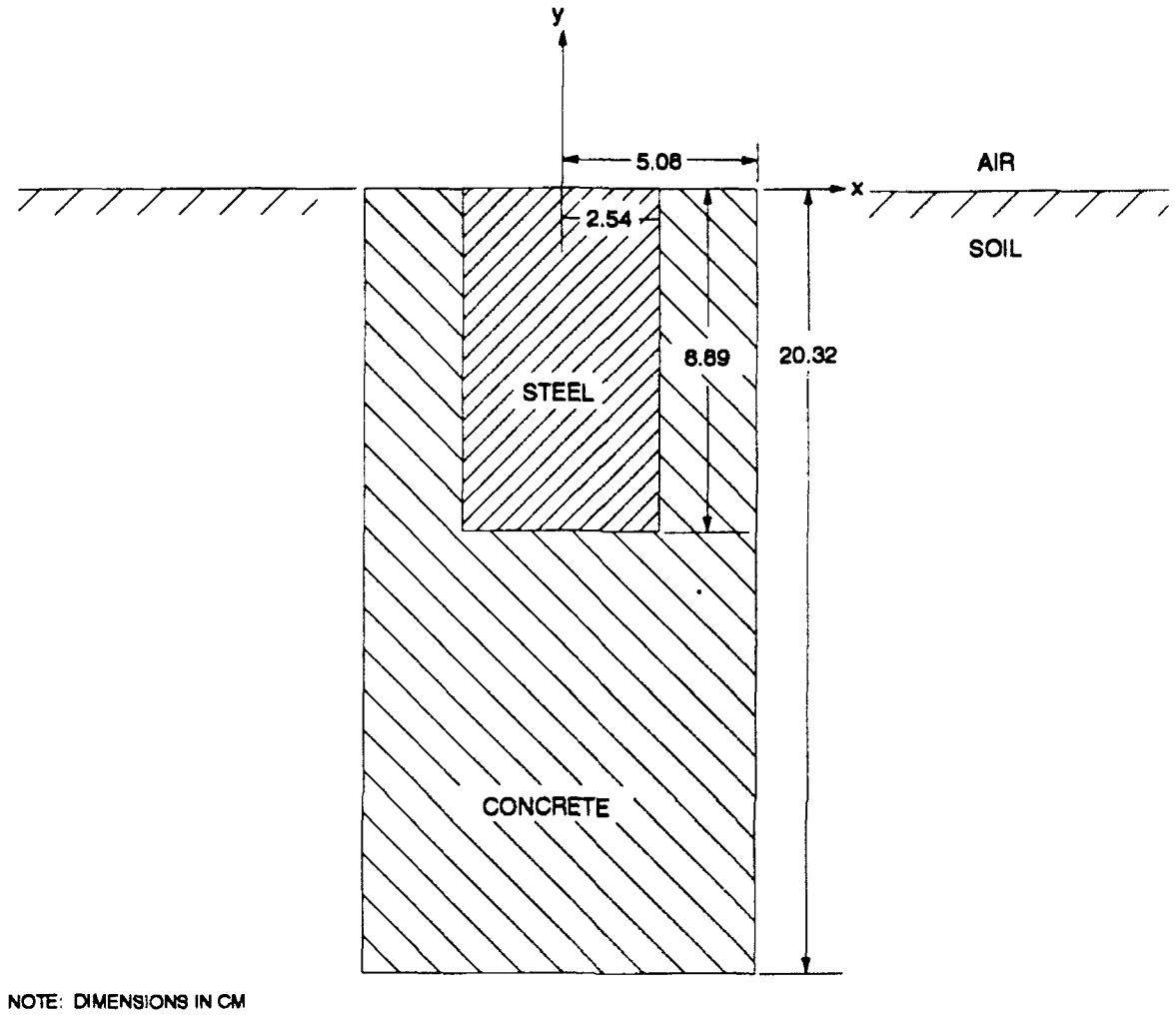

Figure 2. Gage mount for Mineral Find II test.

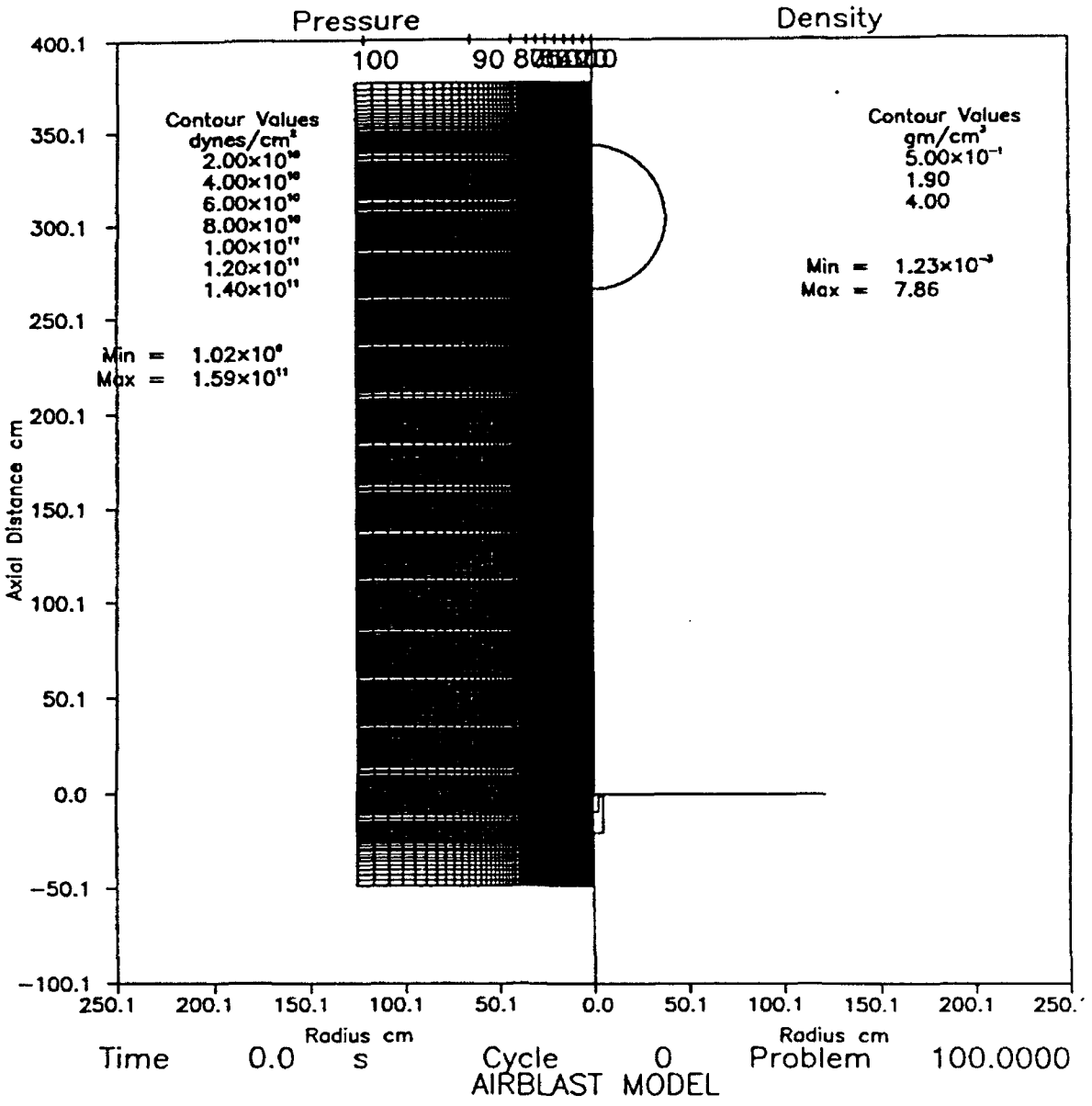

Figure 3. Computational grid.

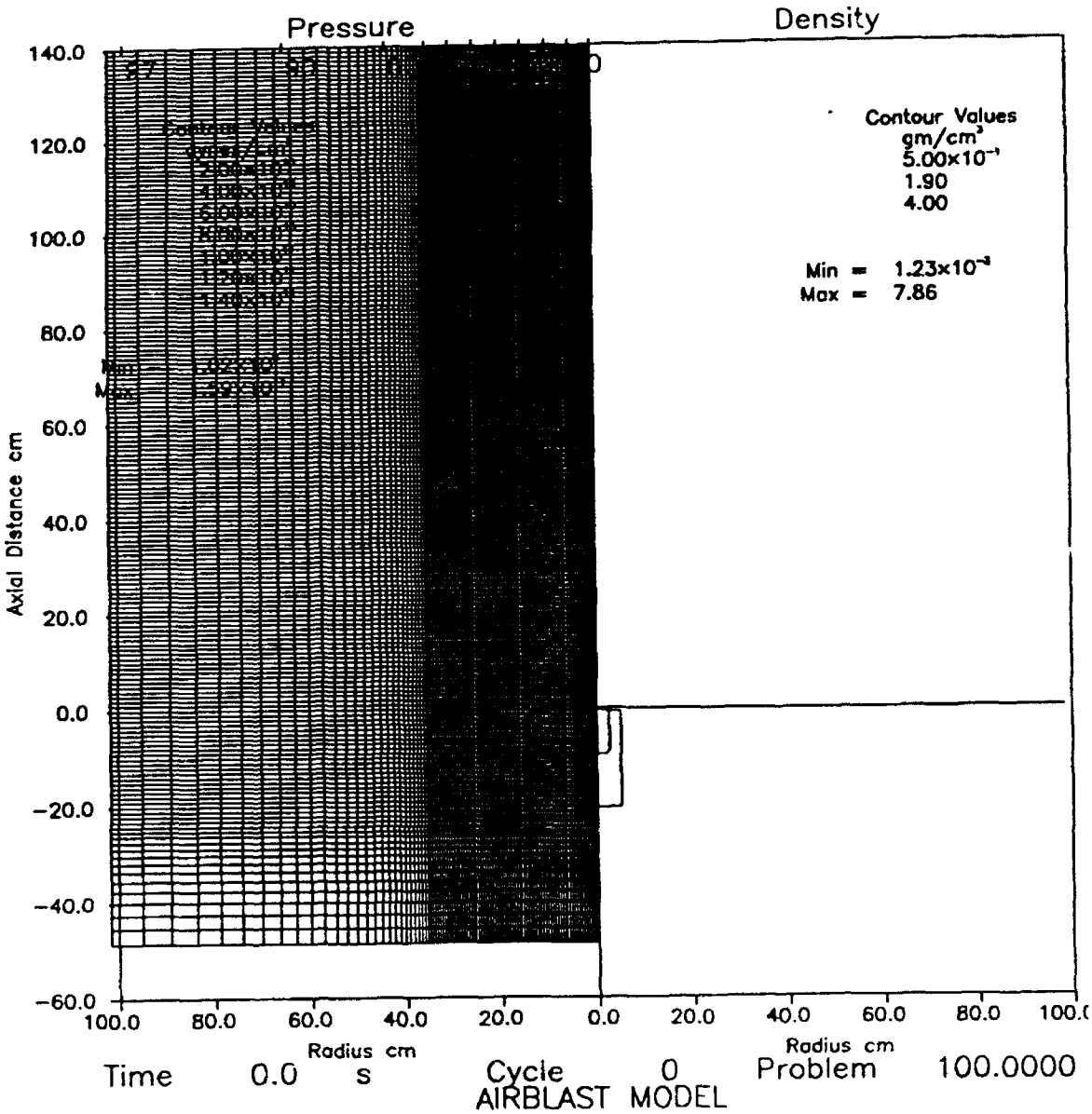

Figure 4. Grid near gage mount.

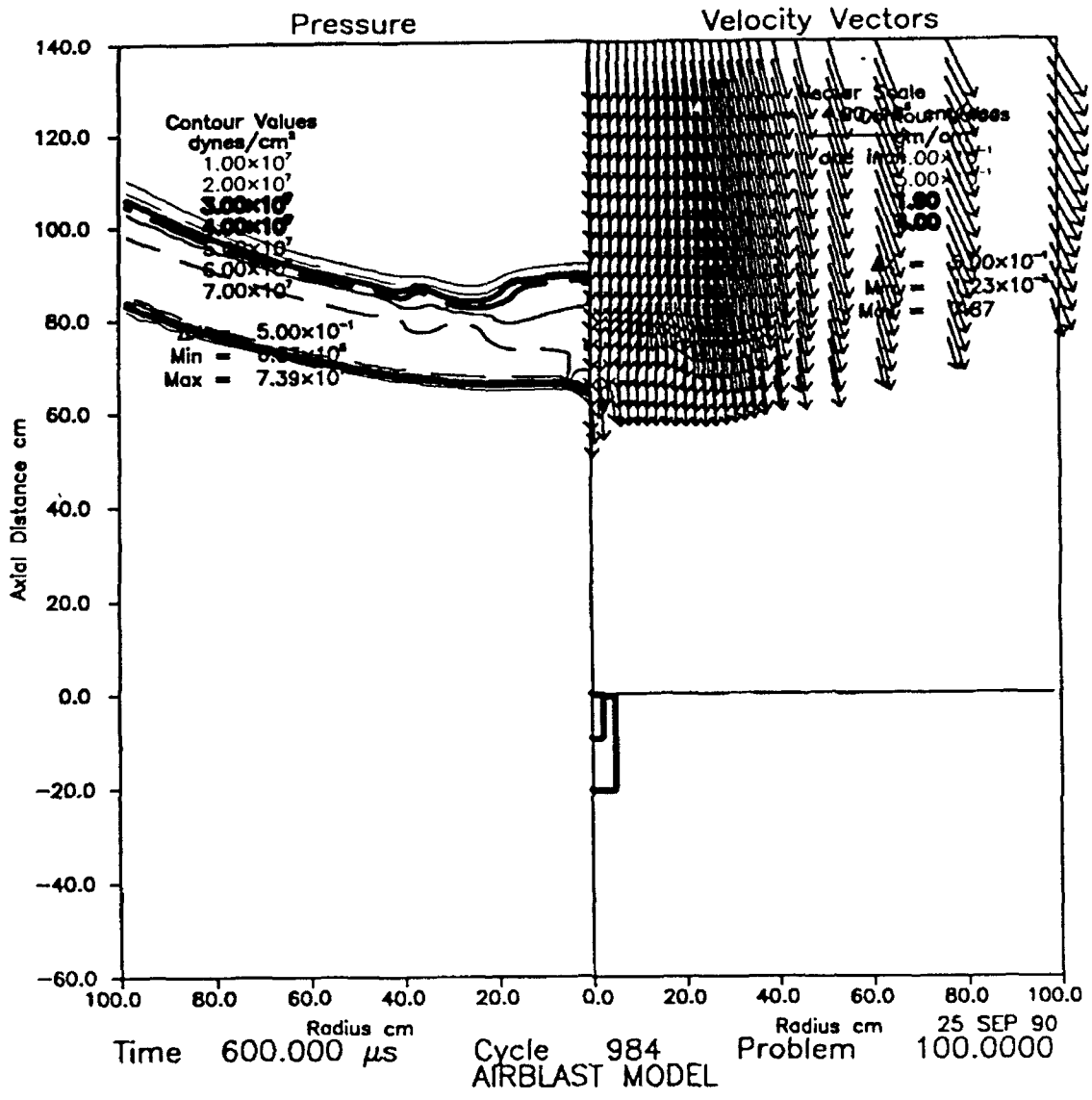

Figure 5. Pressure contours and velocity vectors at t = 0.6 msec.

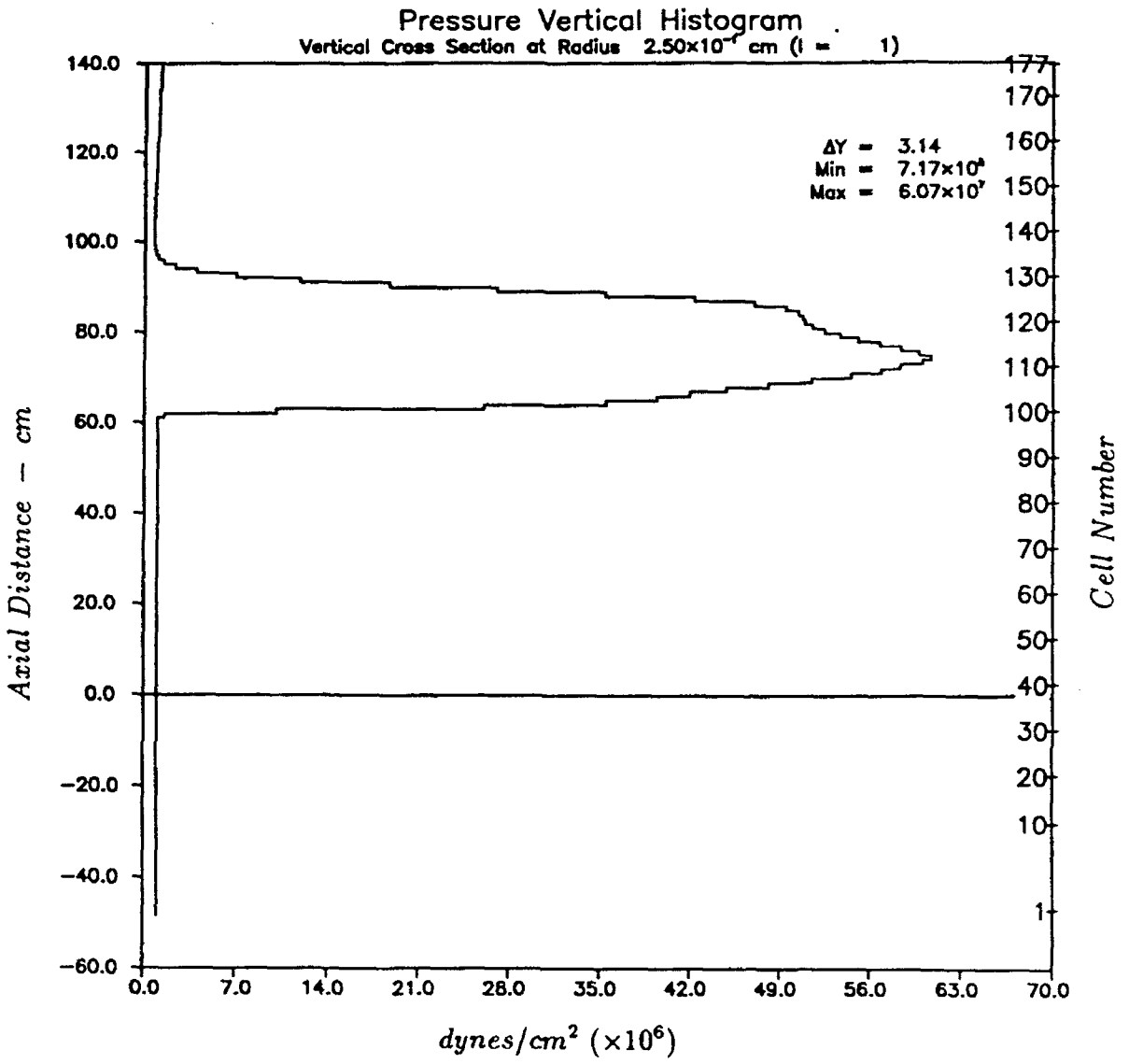

Figure 6. Pressure histogram at t = 0.6 msec.

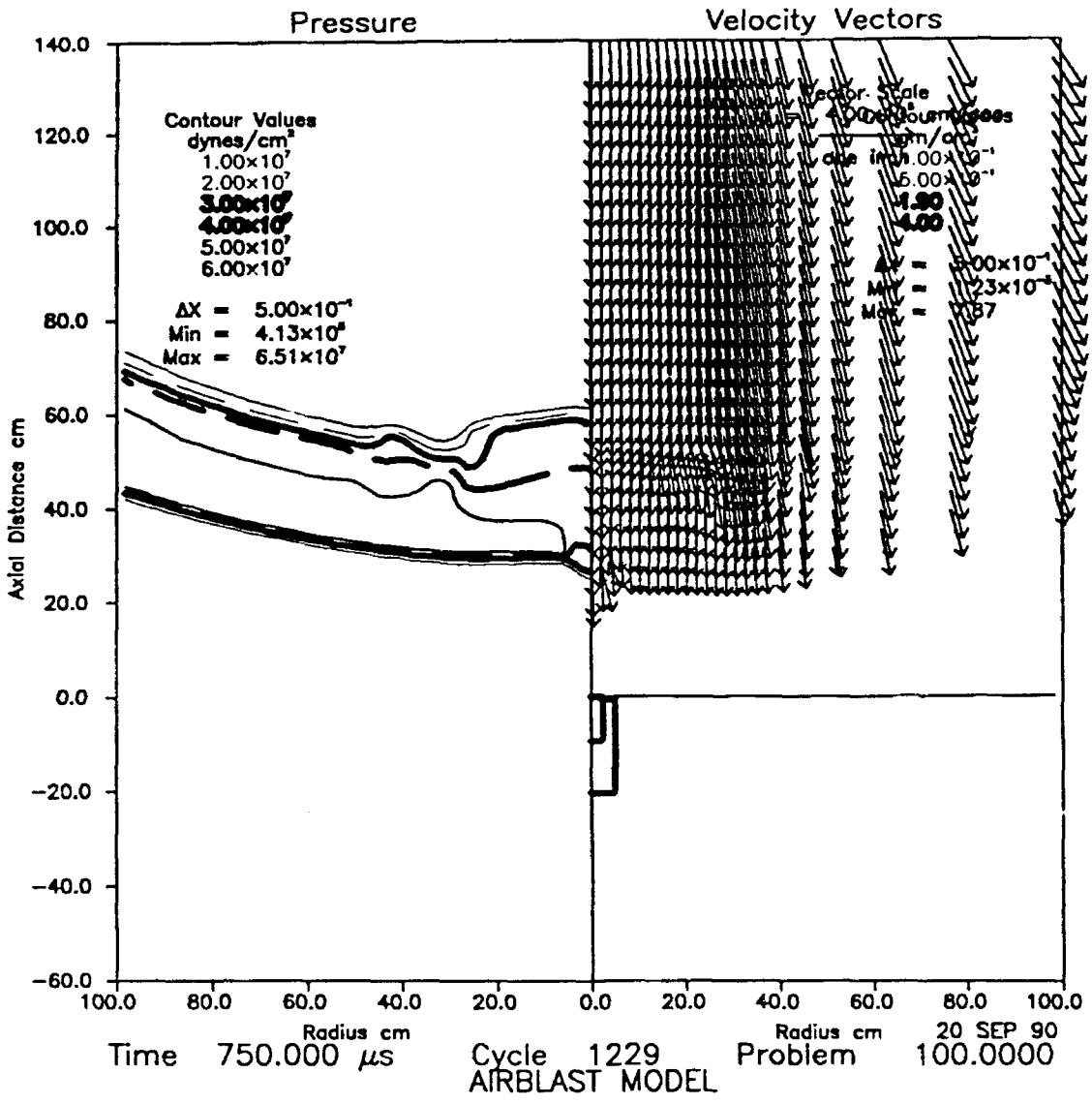

Figure 7. Pressure contours and velocity vectors at t = 0.75 msec.

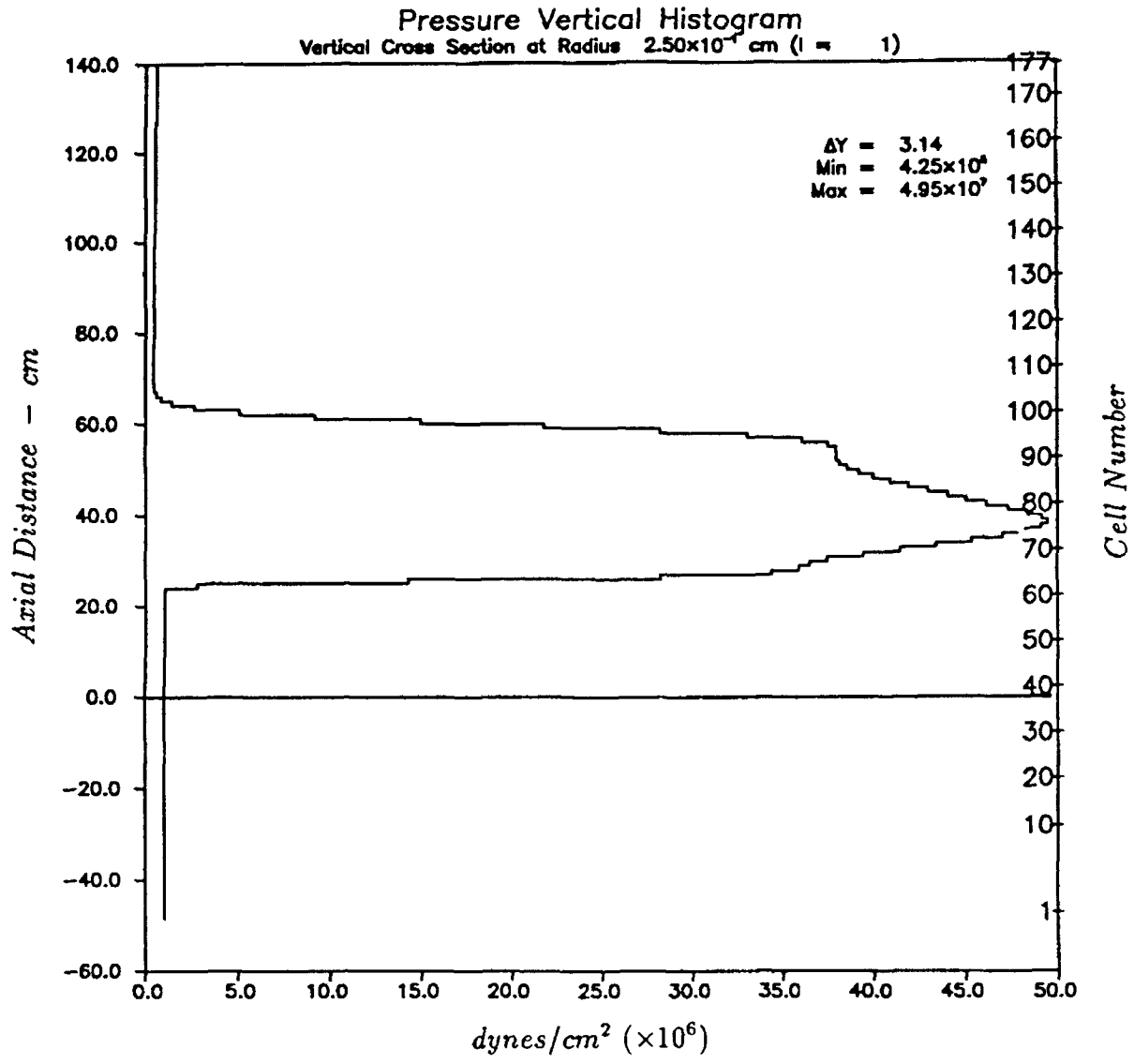

Figure 8. Pressure histogram at t = 0.75 msec.

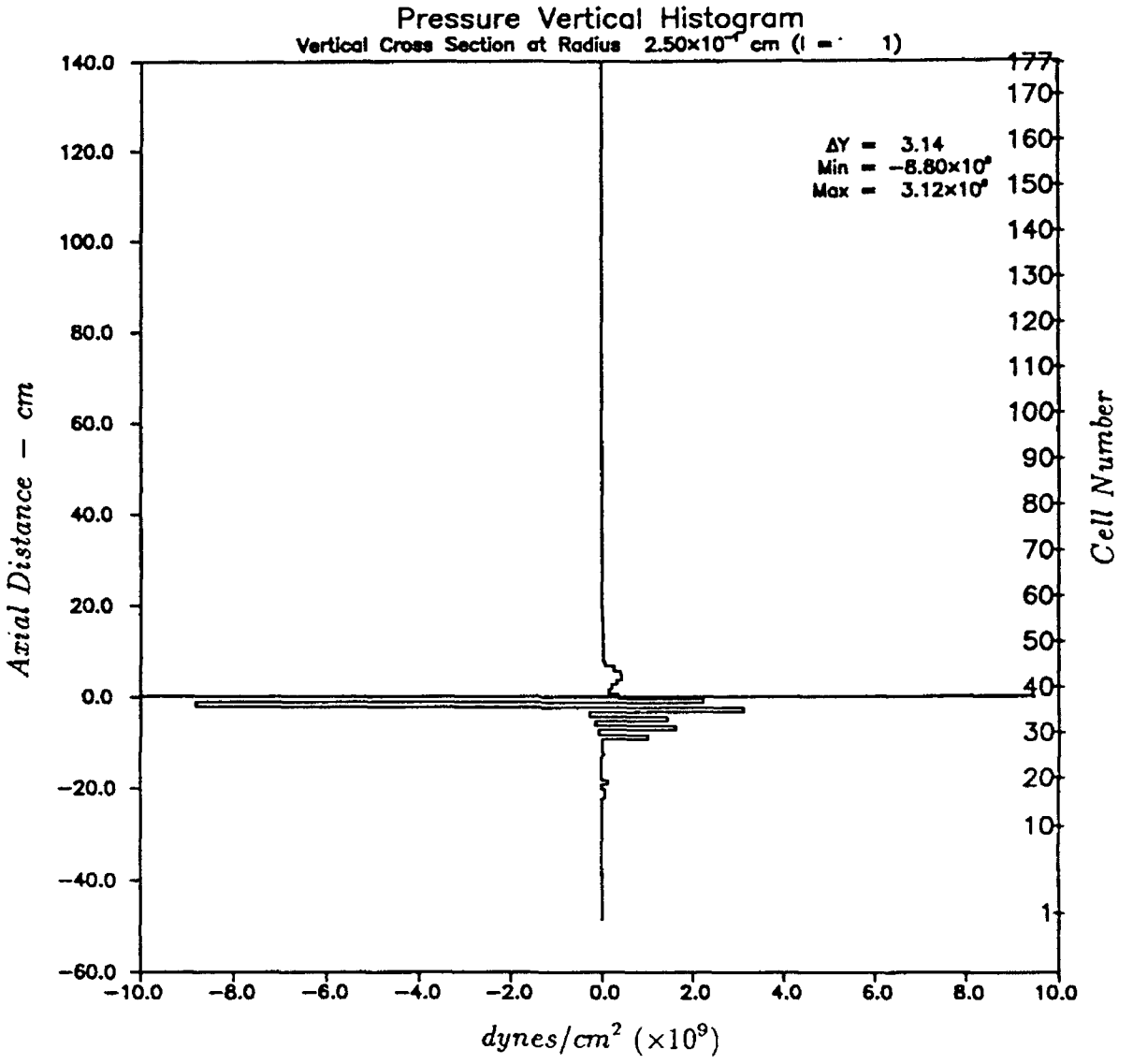

Figure 9. Pressure contours and velocity vectors at t = 1.0 msec, with gage mount included.

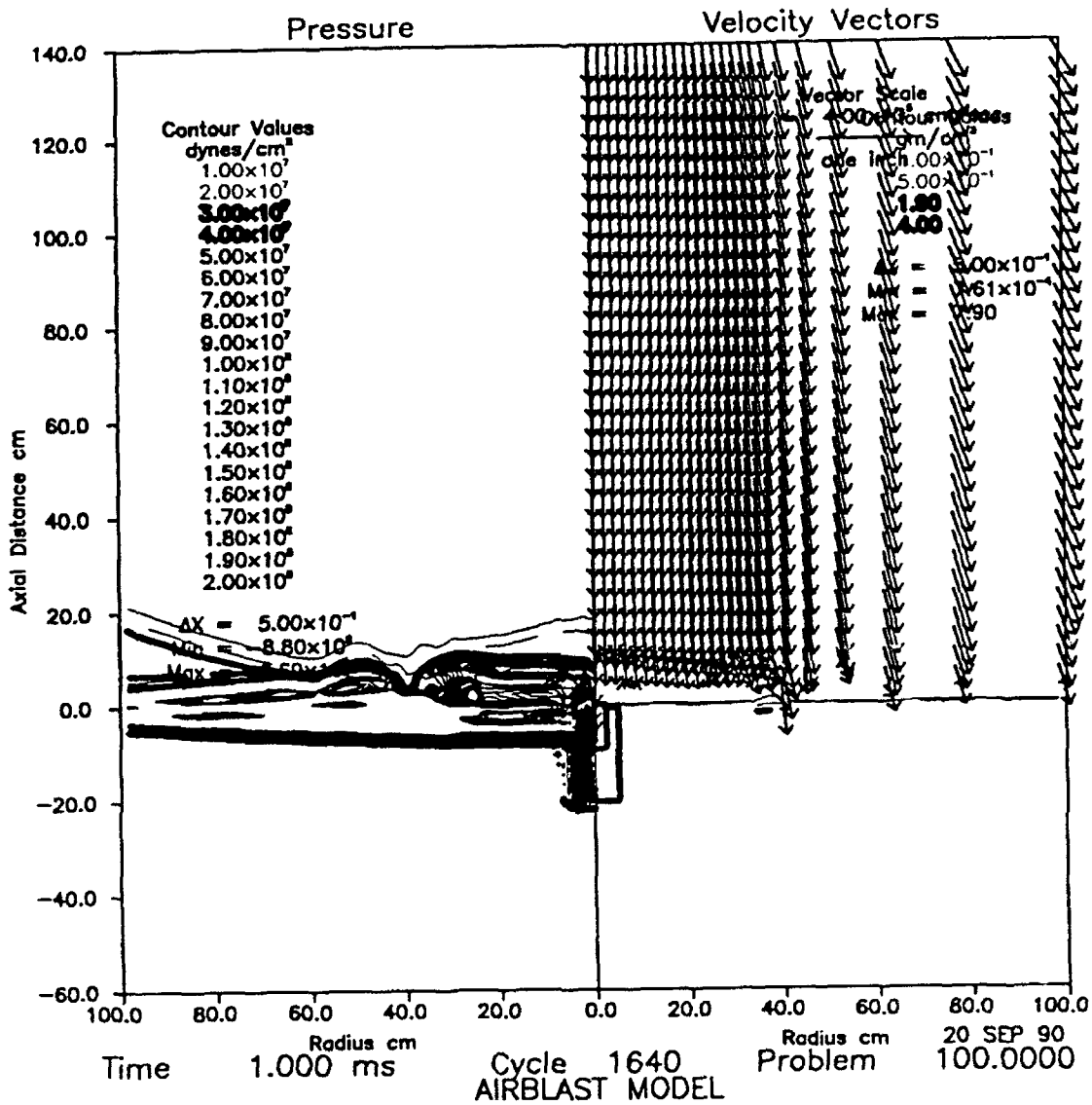

Figure 10. Pressure histogram at t = 1.0 msec, with gage mount included.

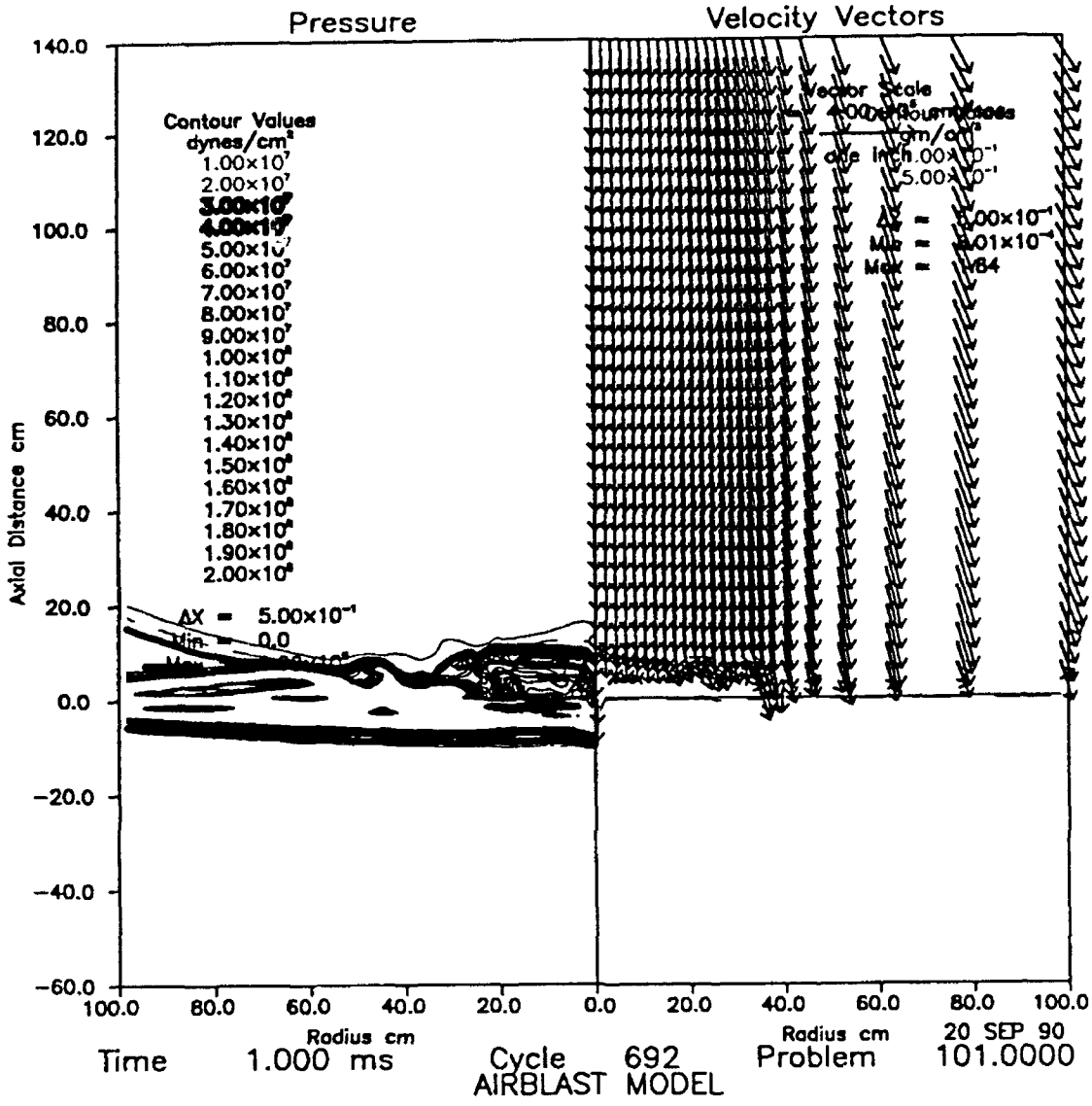

Figure 11. Pressure contours and velocity vectors at t = 1.0 msec, with no gage mount.

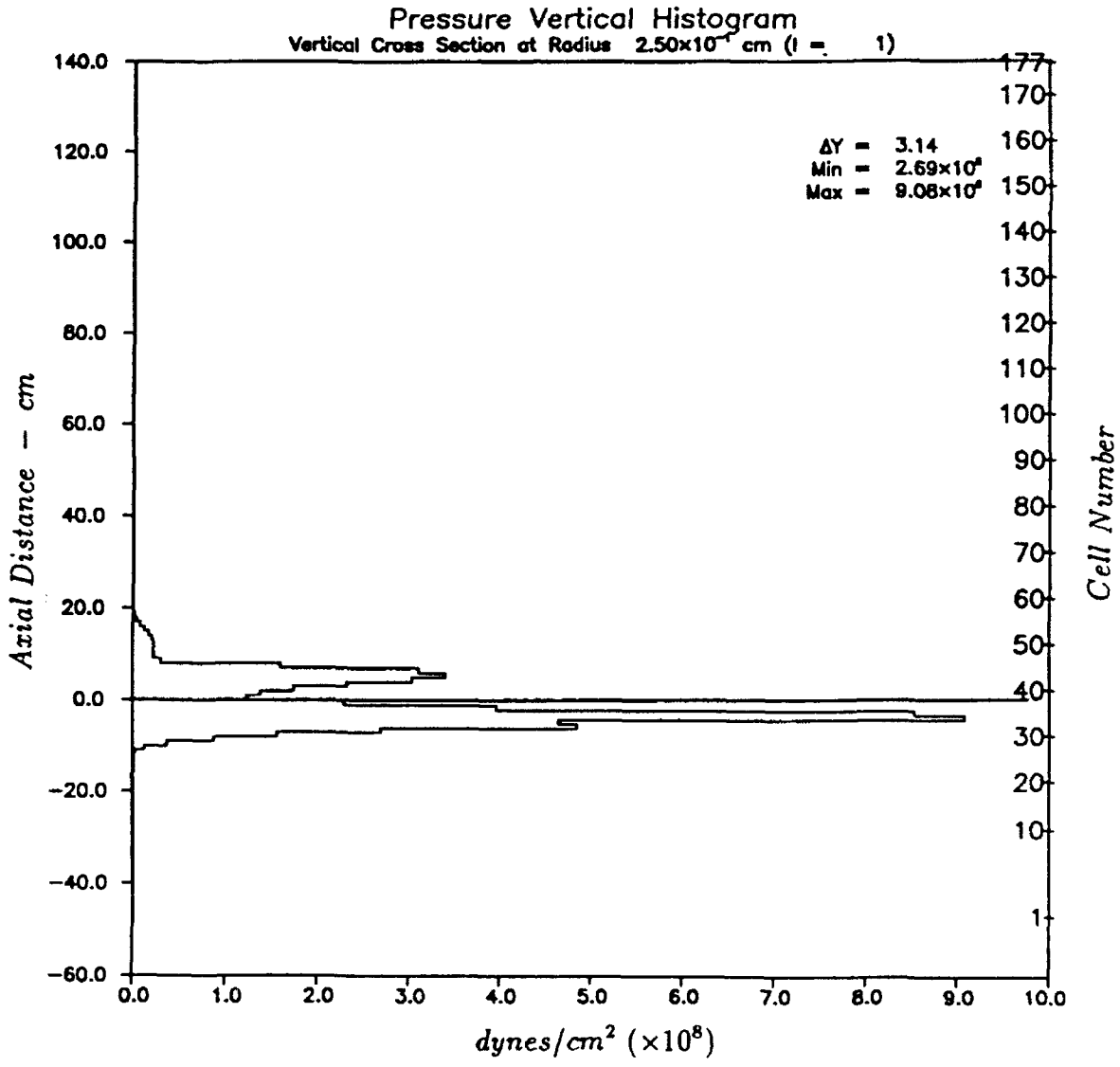

Figure 12. Pressure histogram at t = 1.0 msec,
with no gage mount.

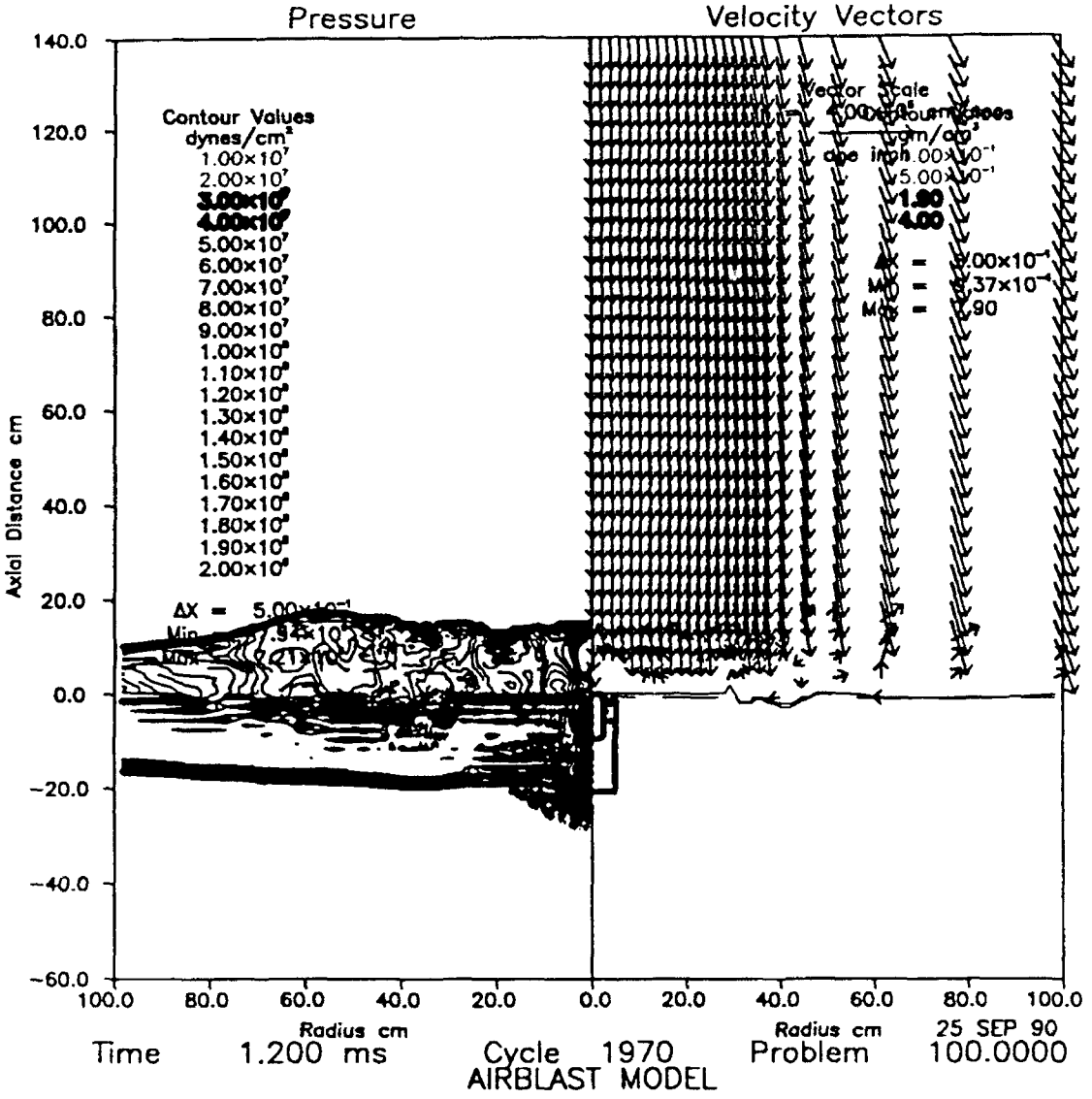

Figure 13. Pressure contours and velocity vectors at t = 1.2 msec, with gage mount included.

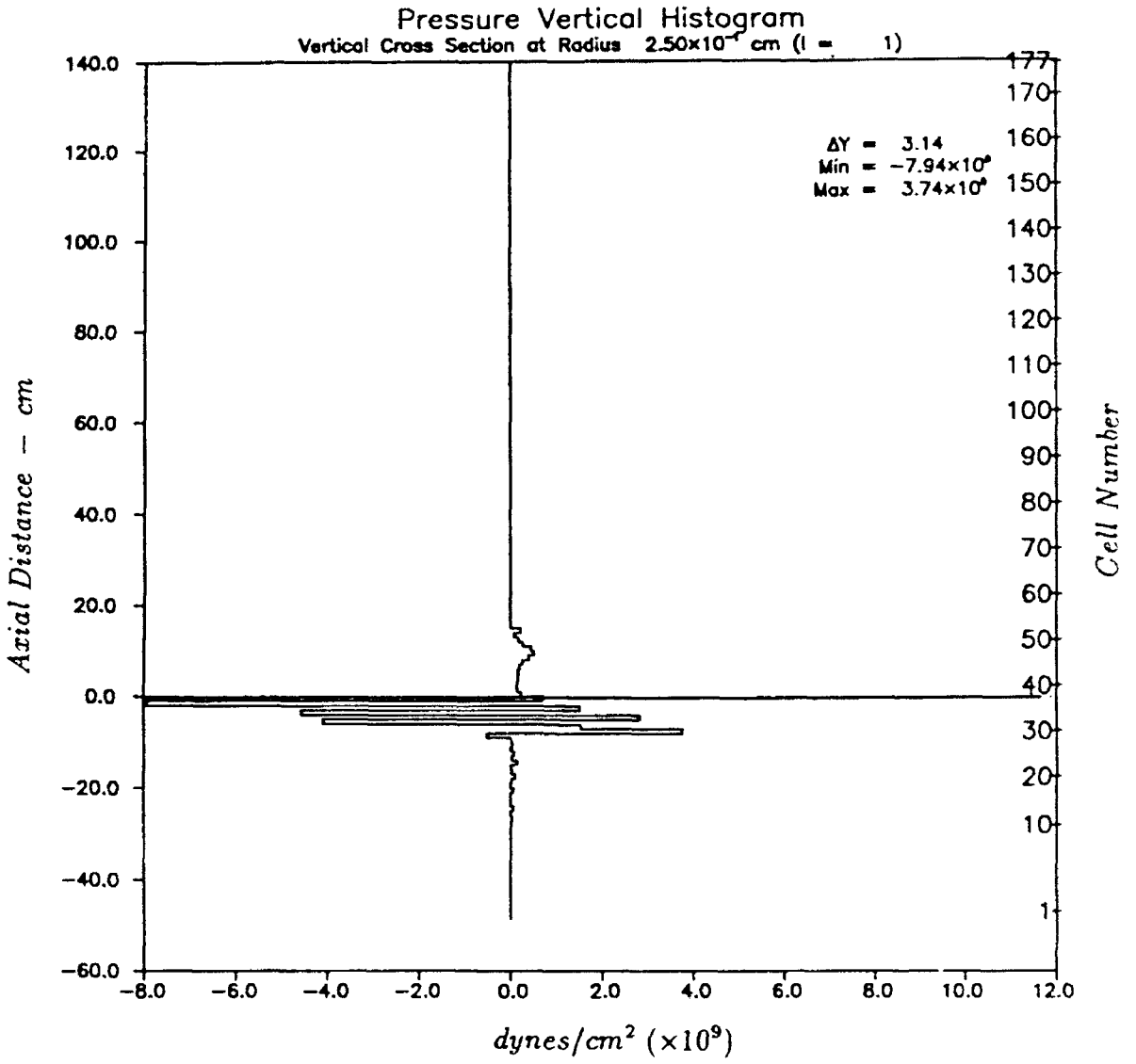

Figure 14. Pressure histogram at t = 1.2 msec,
with gage mount included.

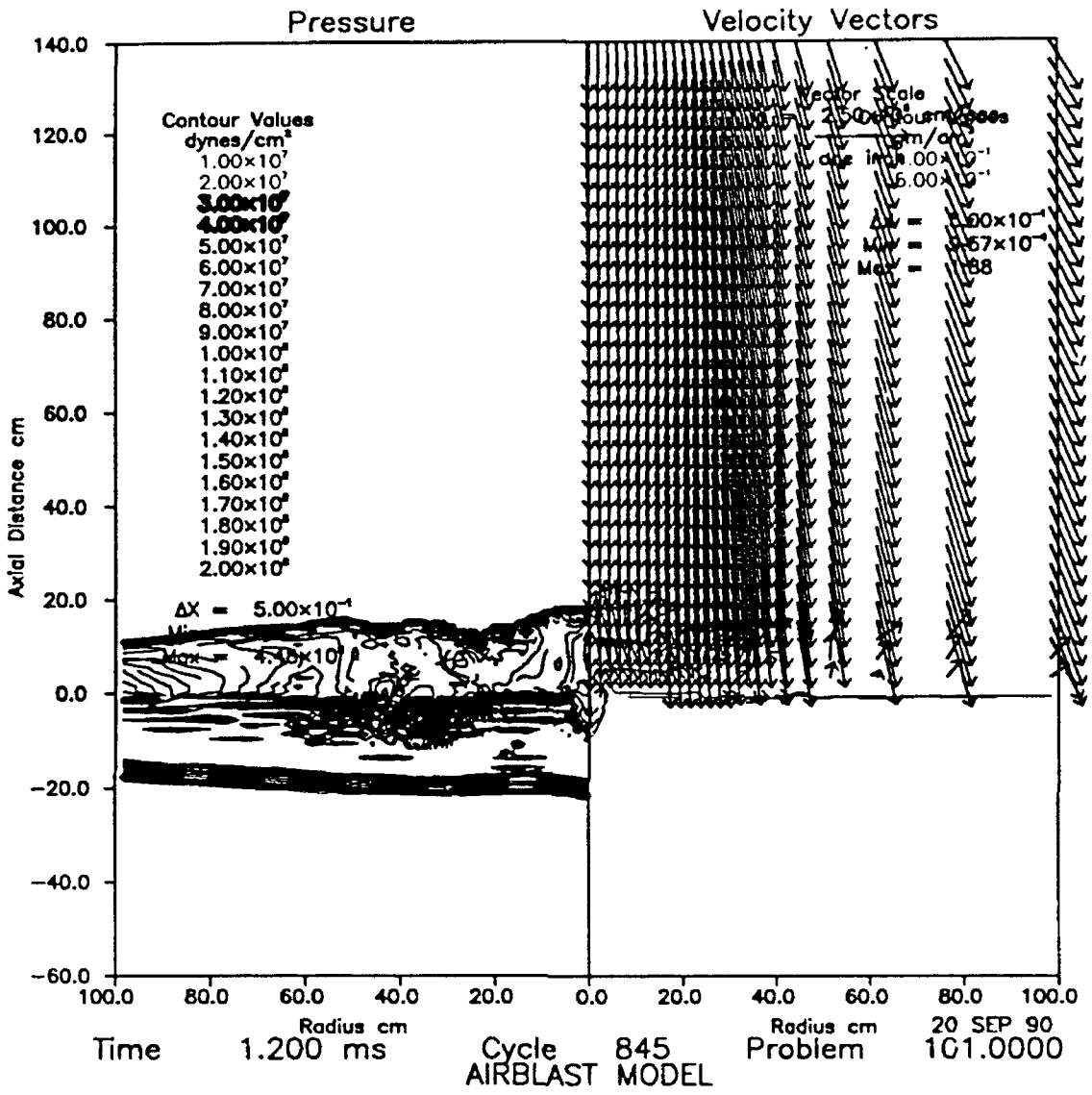

Figure 15. Pressure contours and velocity vectors at t = 1.2 msec, with no gage mount.

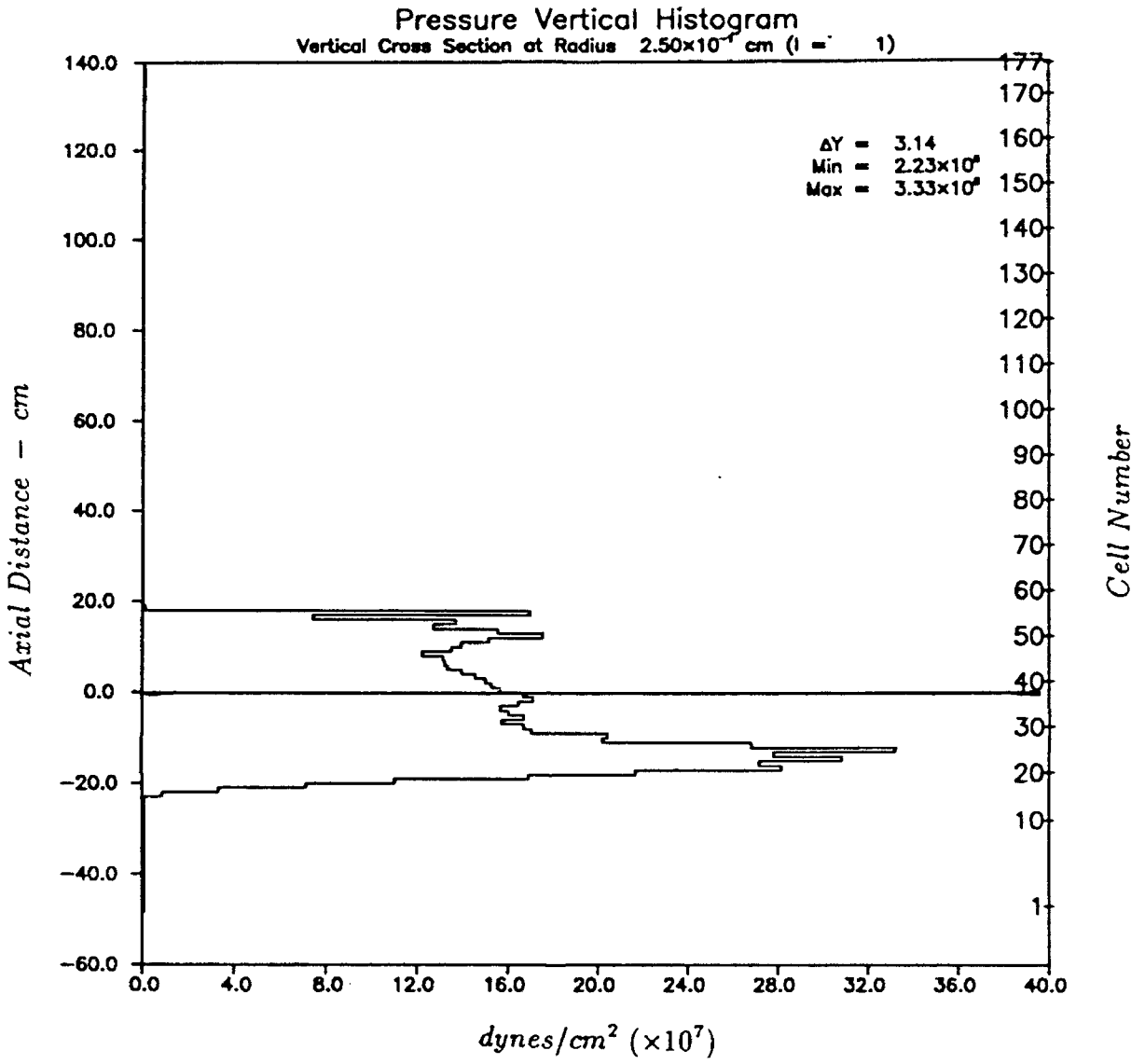

Figure 16. Pressure histogram at t = 1.2 msec,
with no gage mount.

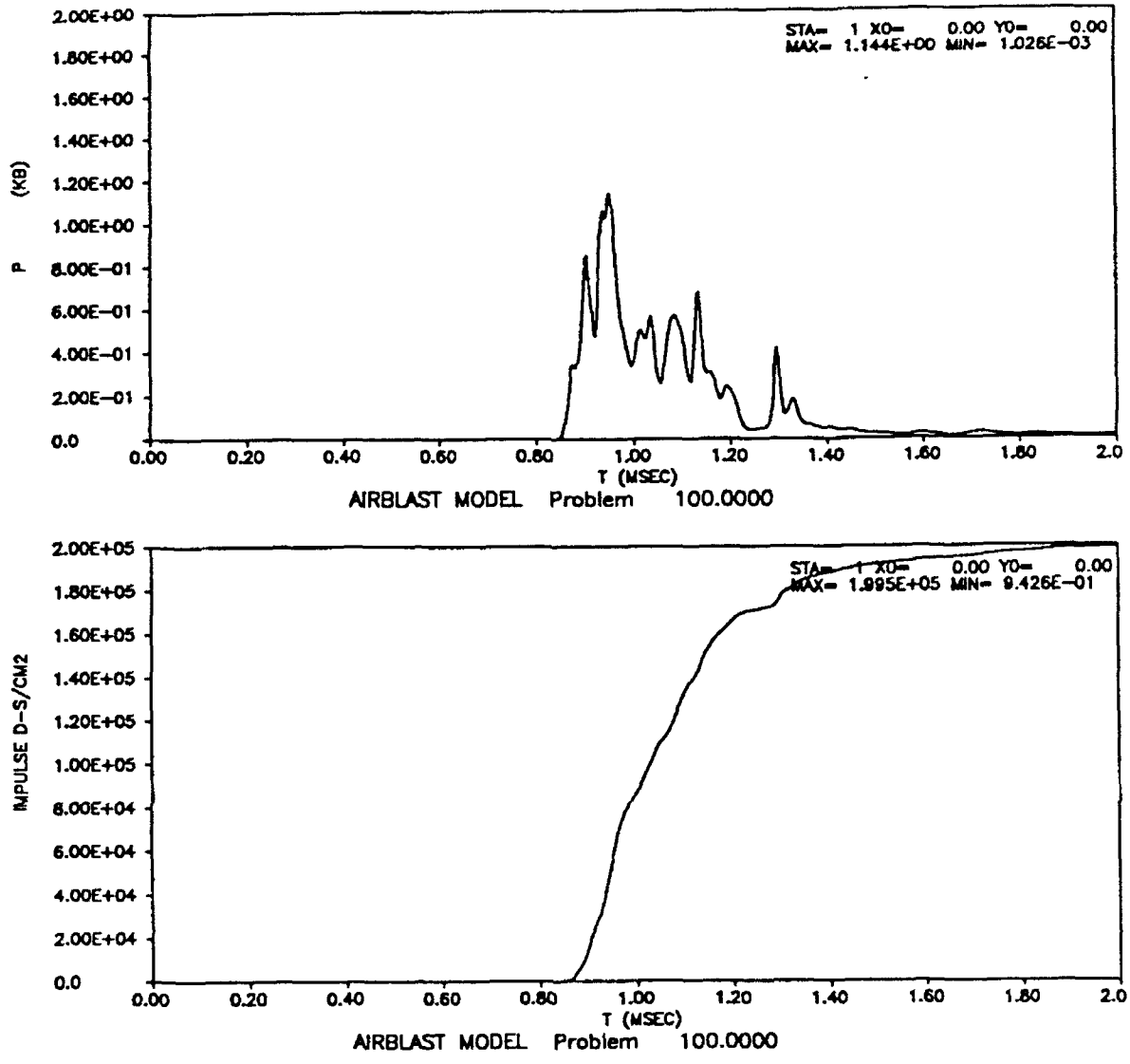

Figure 17. Pressure time history at ground zero, on top of steel cylinder in gage mount.

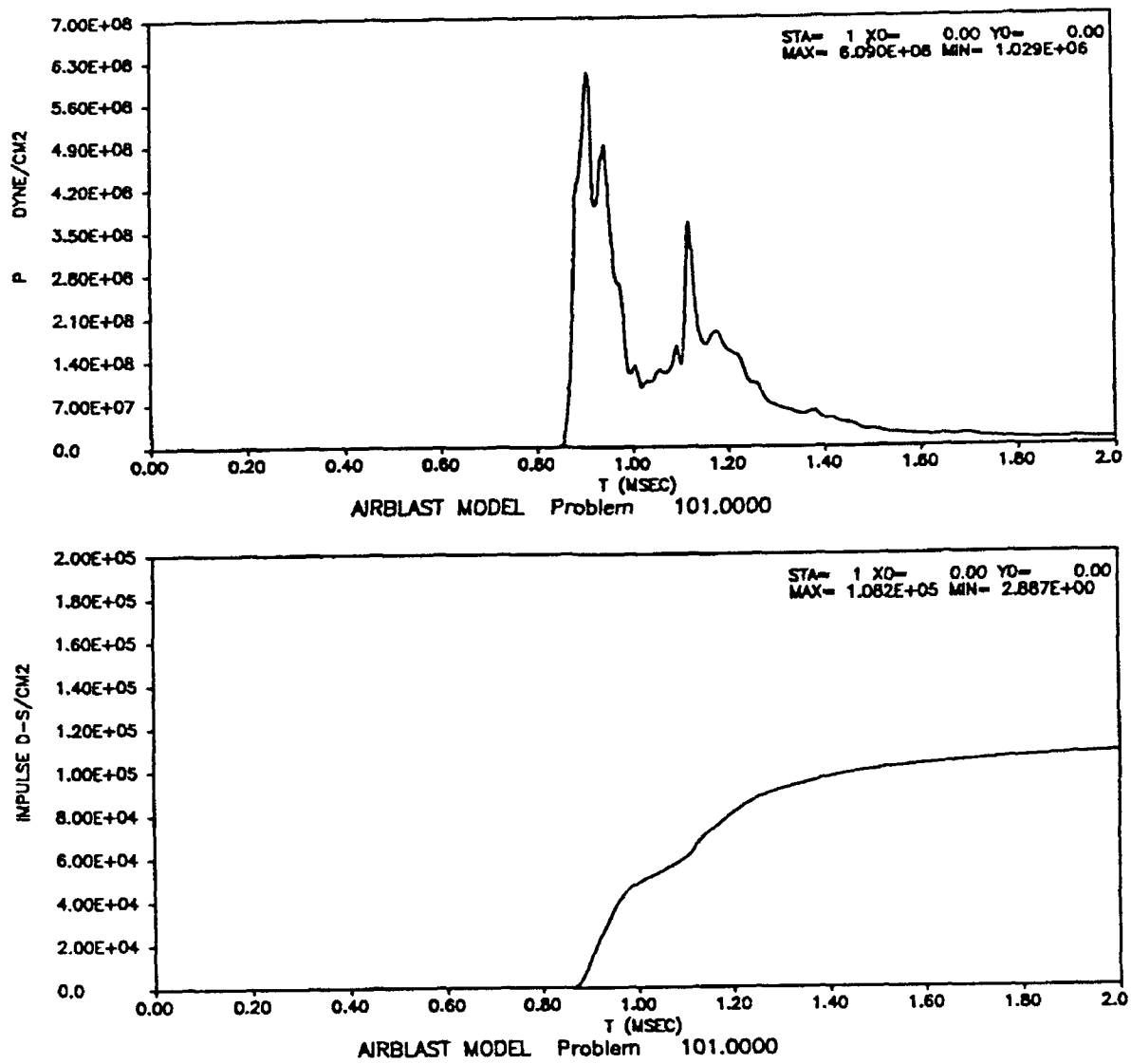

Figure 18. Pressure time history at ground zero, in free-field (no gage mount).

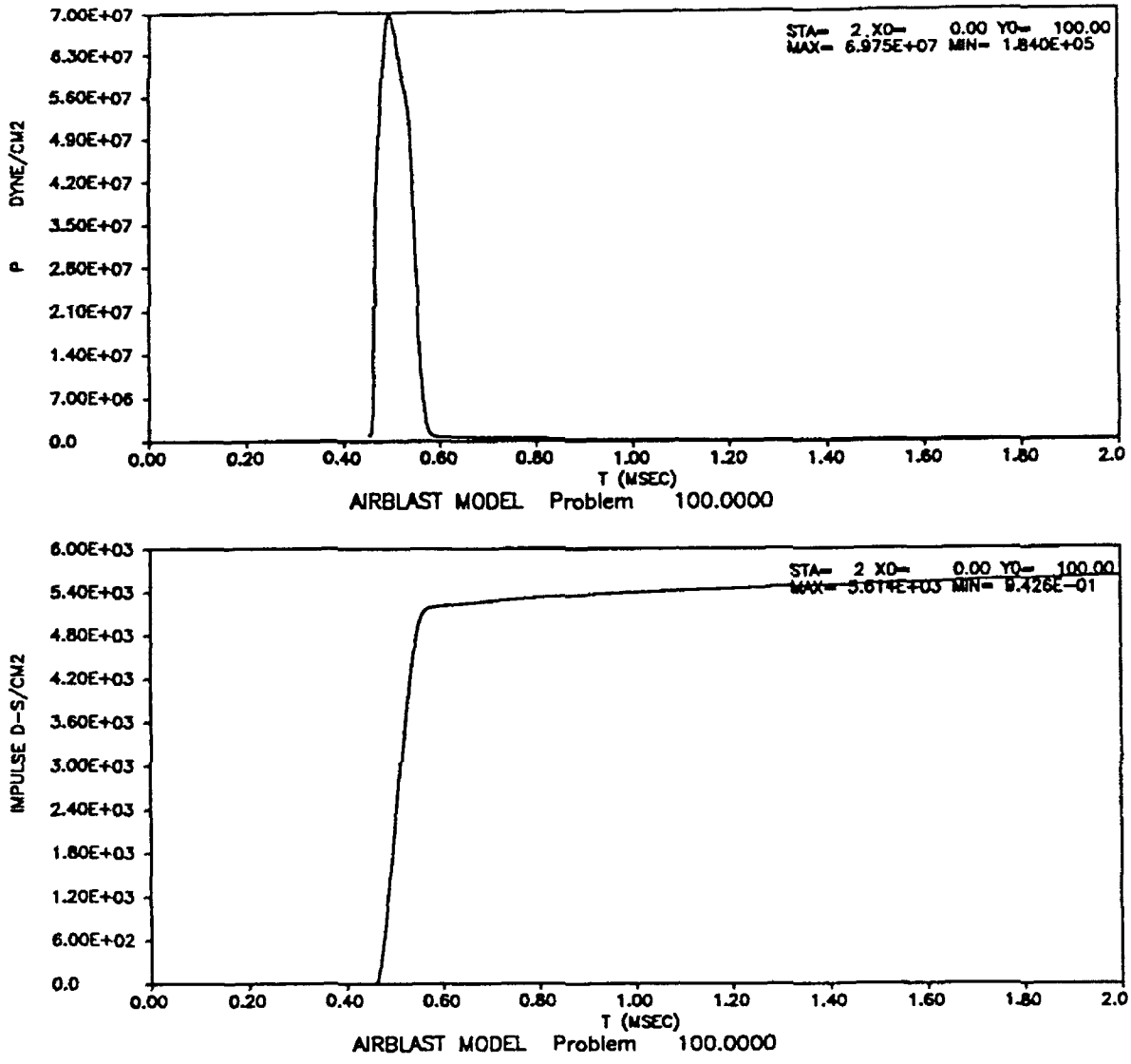

Figure 19. Pressure time history at 100 cm above ground zero.

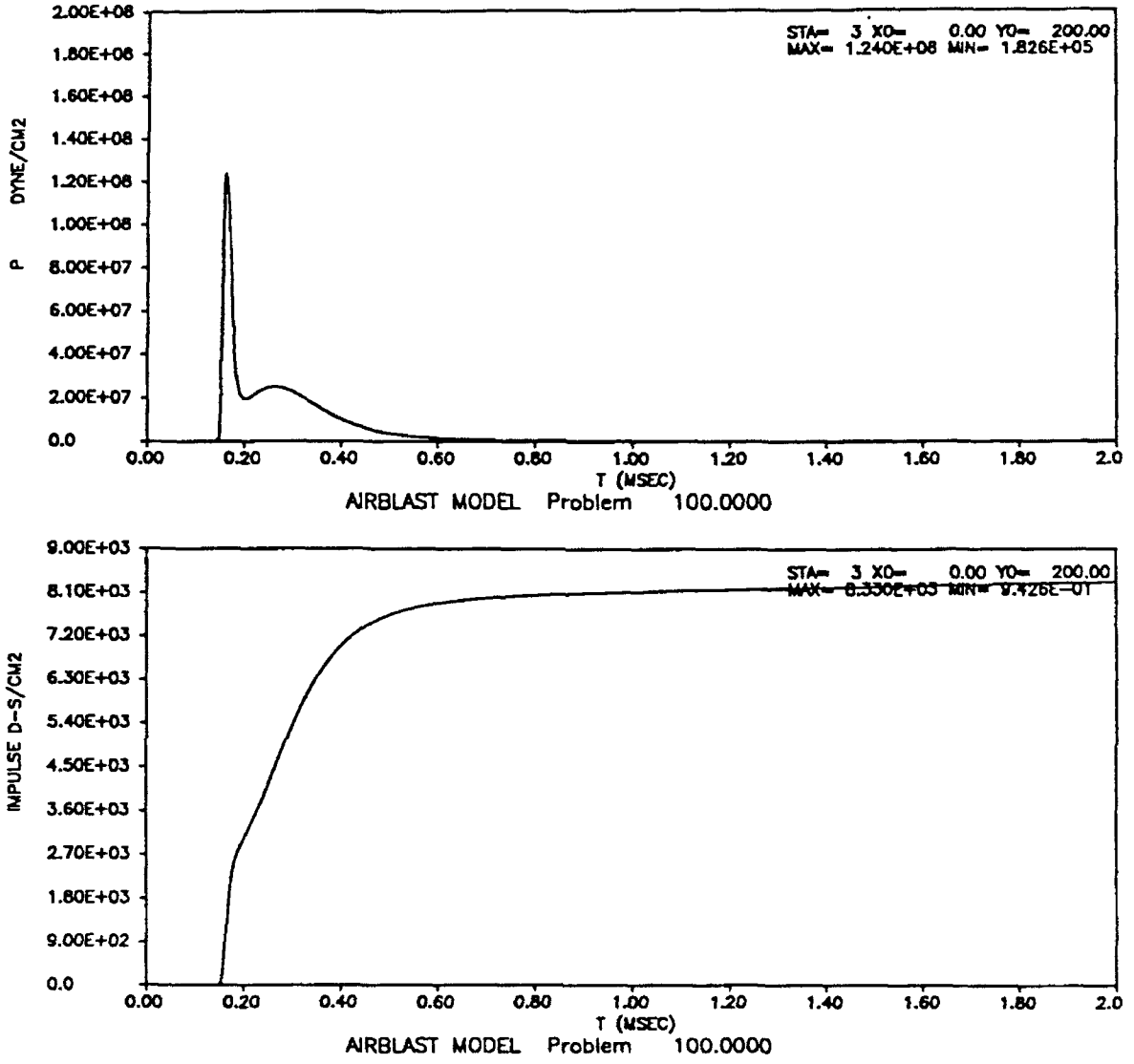

Figure 20. Pressure time history at 200 cm above ground zero.

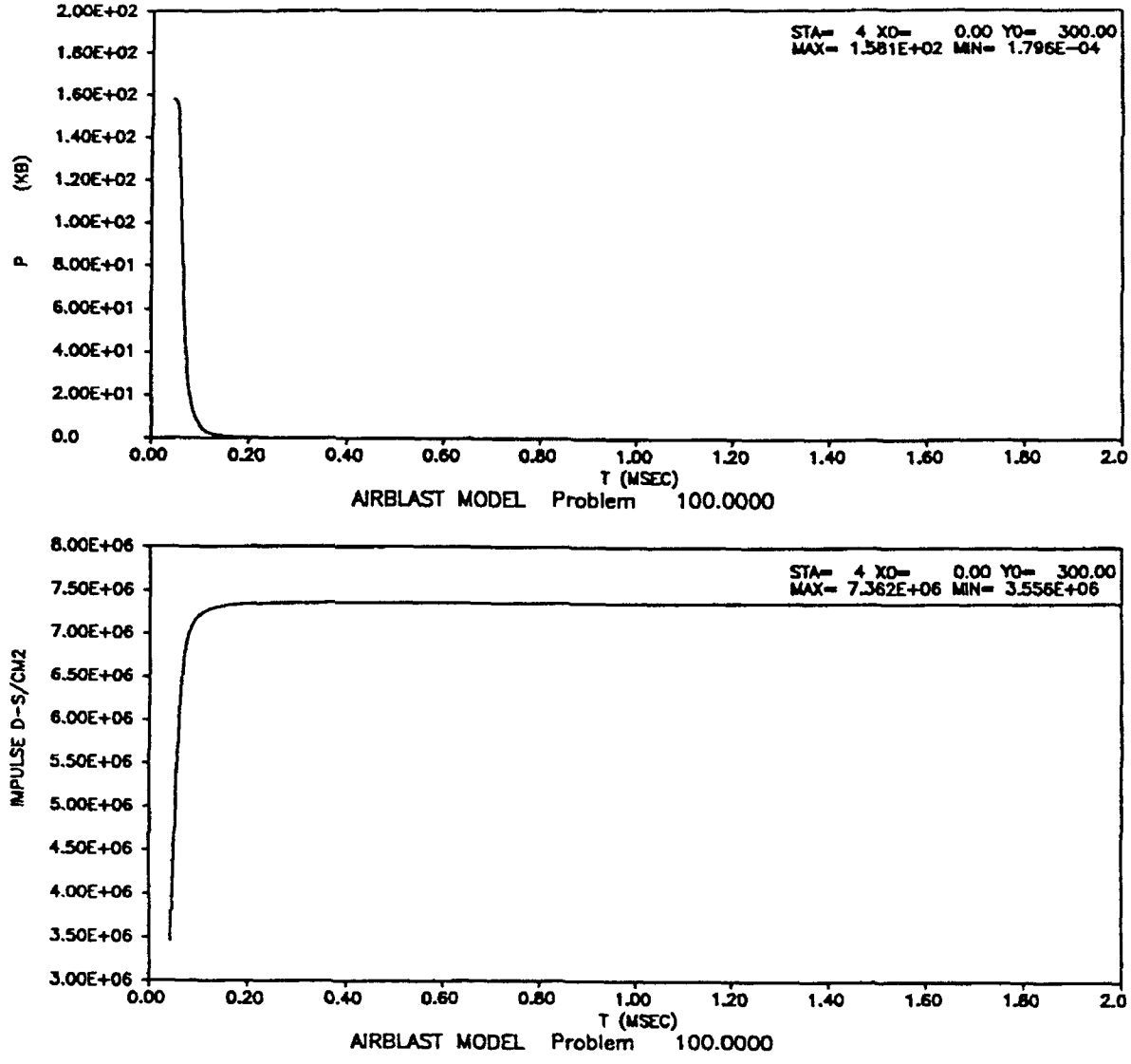

Figure 21. Pressure time history near surface of charge.

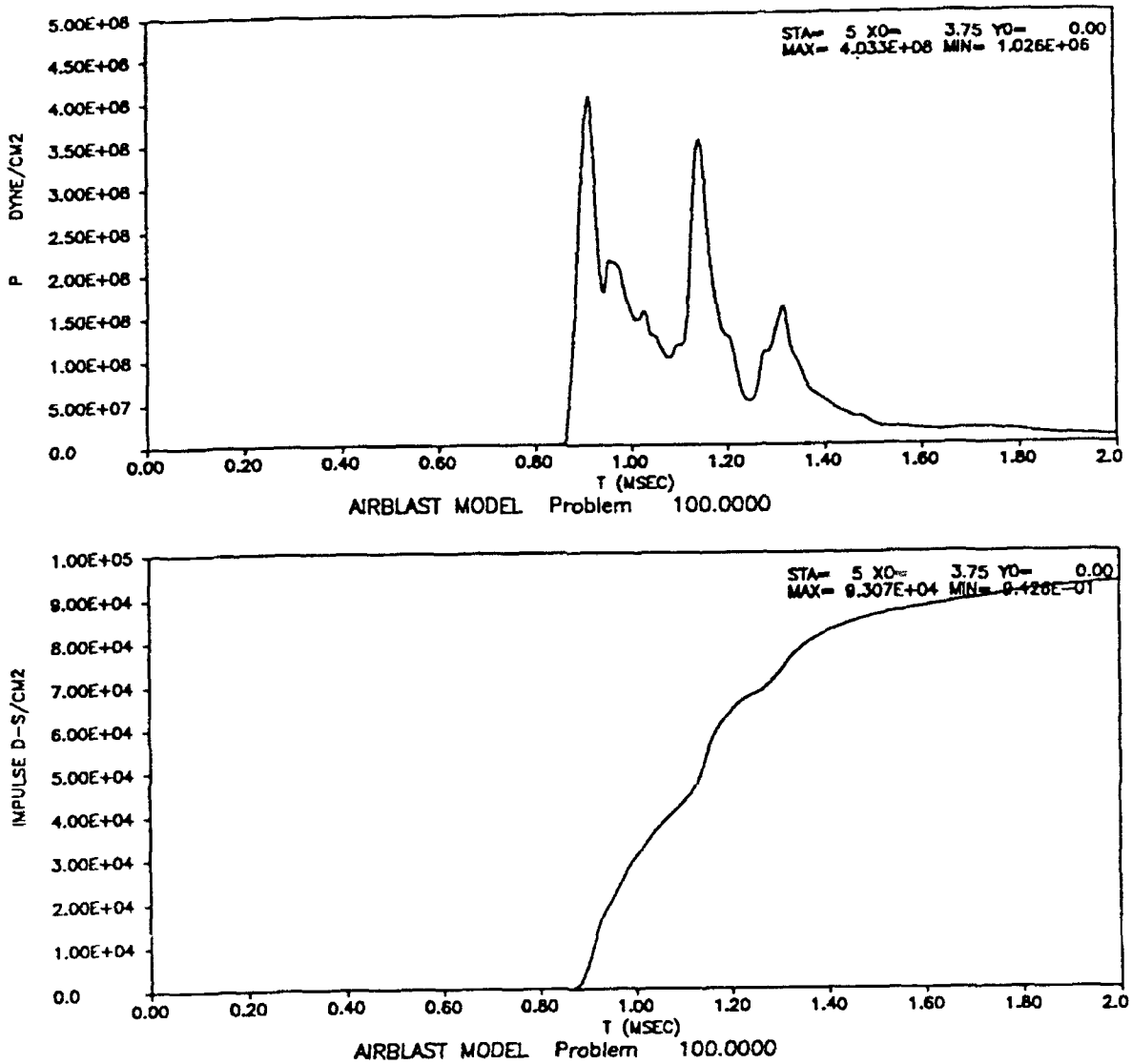

Figure 22. Pressure time history at 3.75-cm ground range, on concrete ring of gage mount.

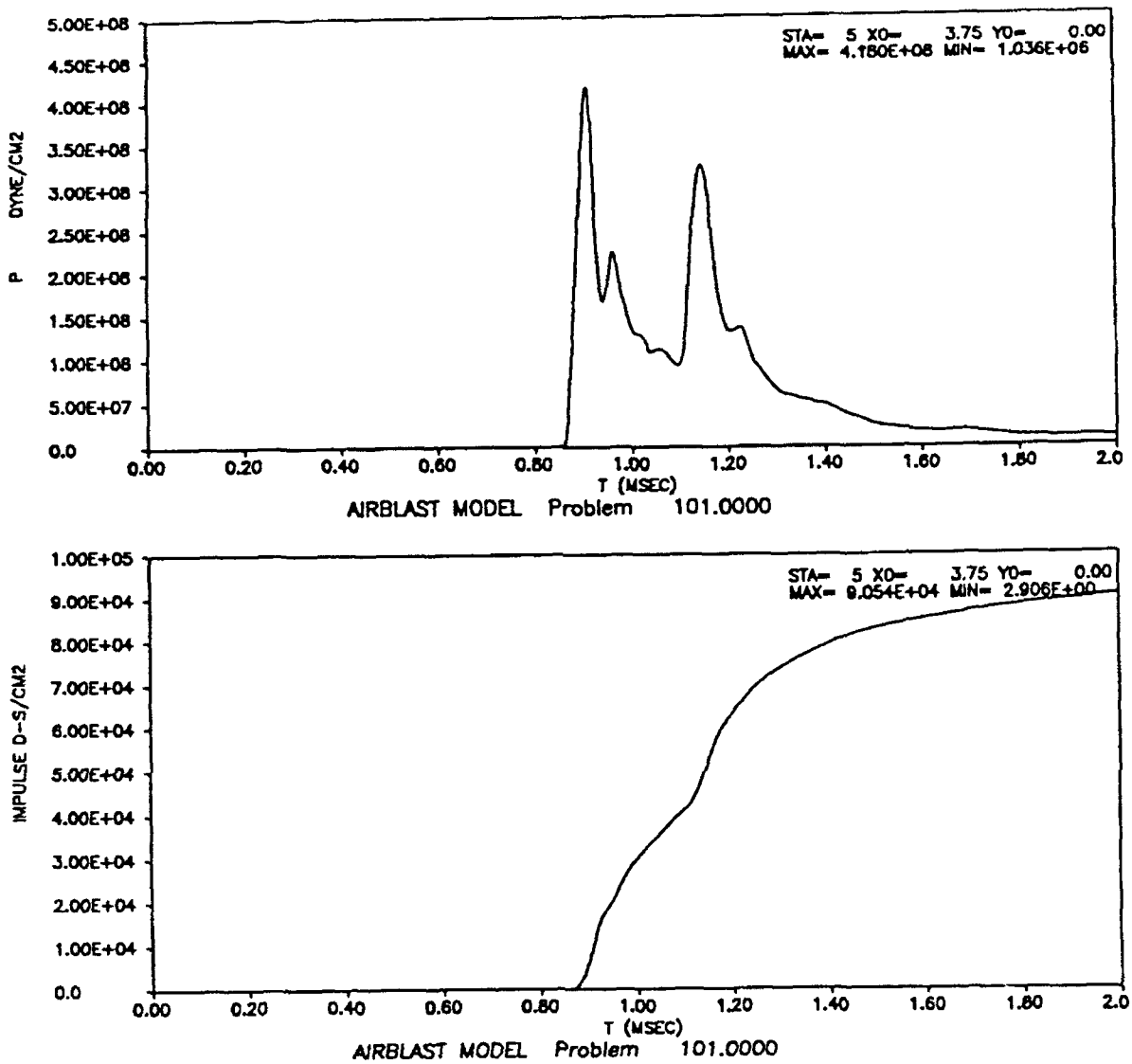

Figure 23. Pressure time history at 3.75-cm ground range, with no gage mount.

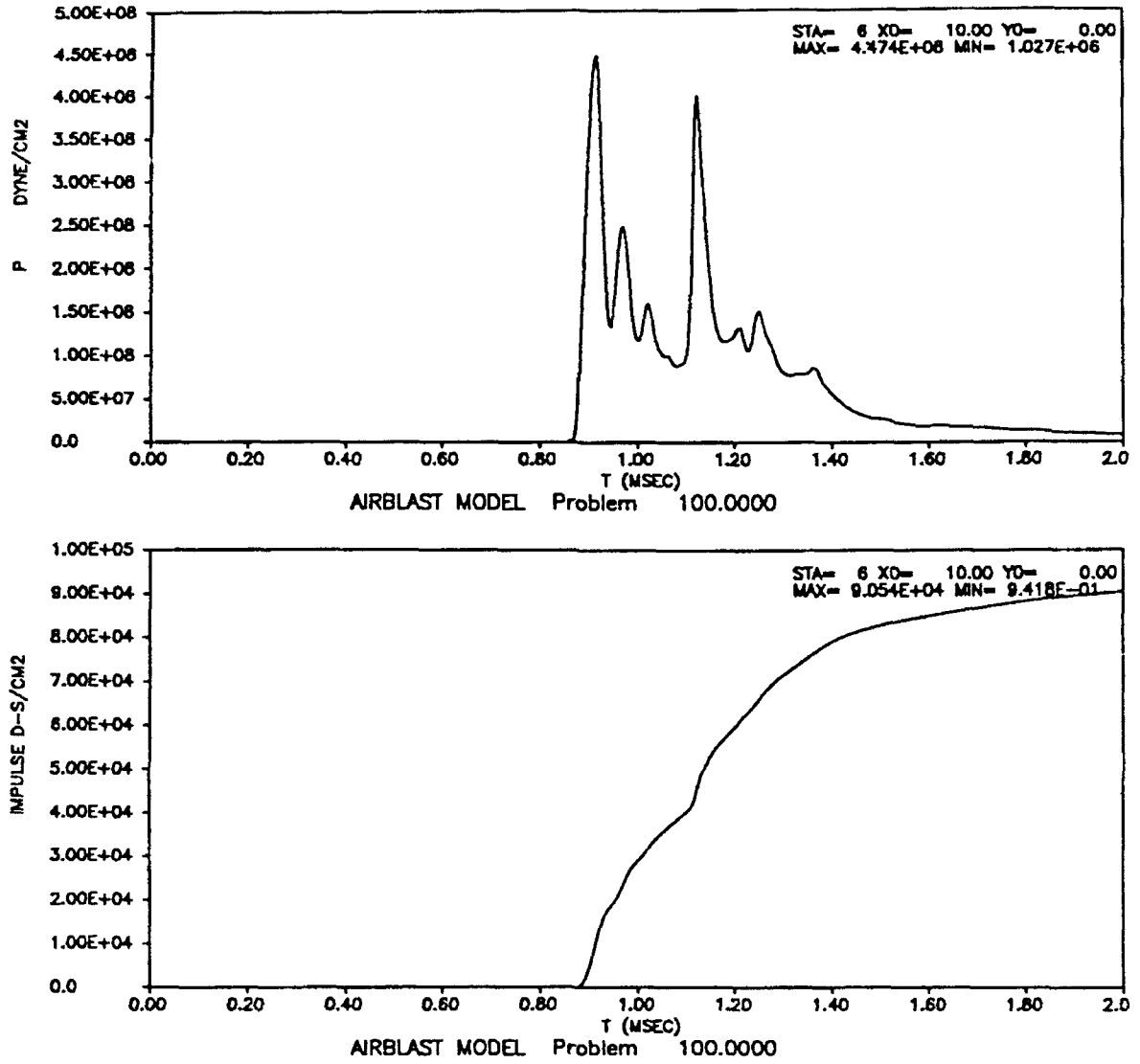

Figure 24. Pressure time history at 10.0-cm ground range, with gage mount included.

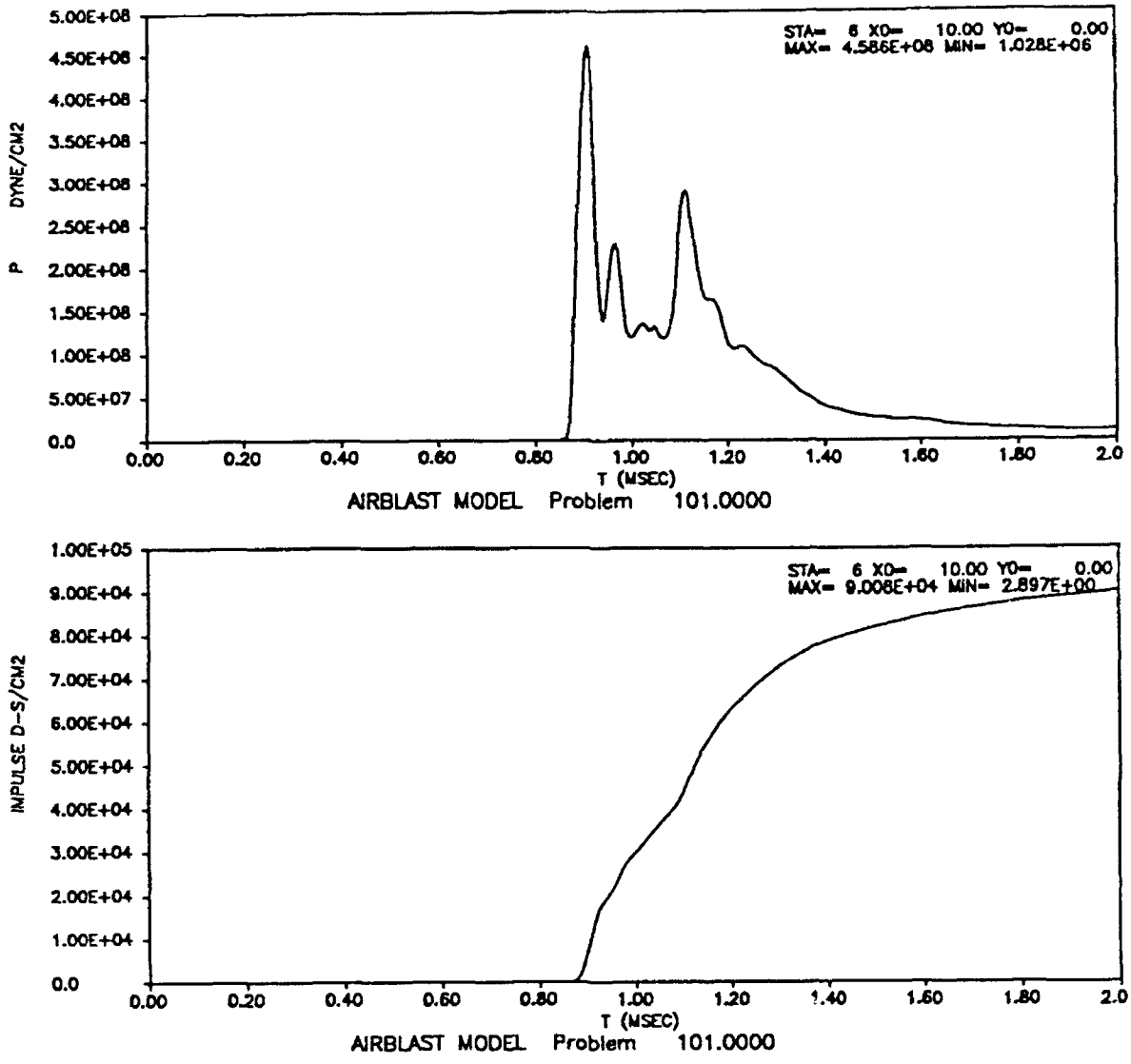

Figure 25. Pressure time history at 10.0-cm ground range, with no gage mount.

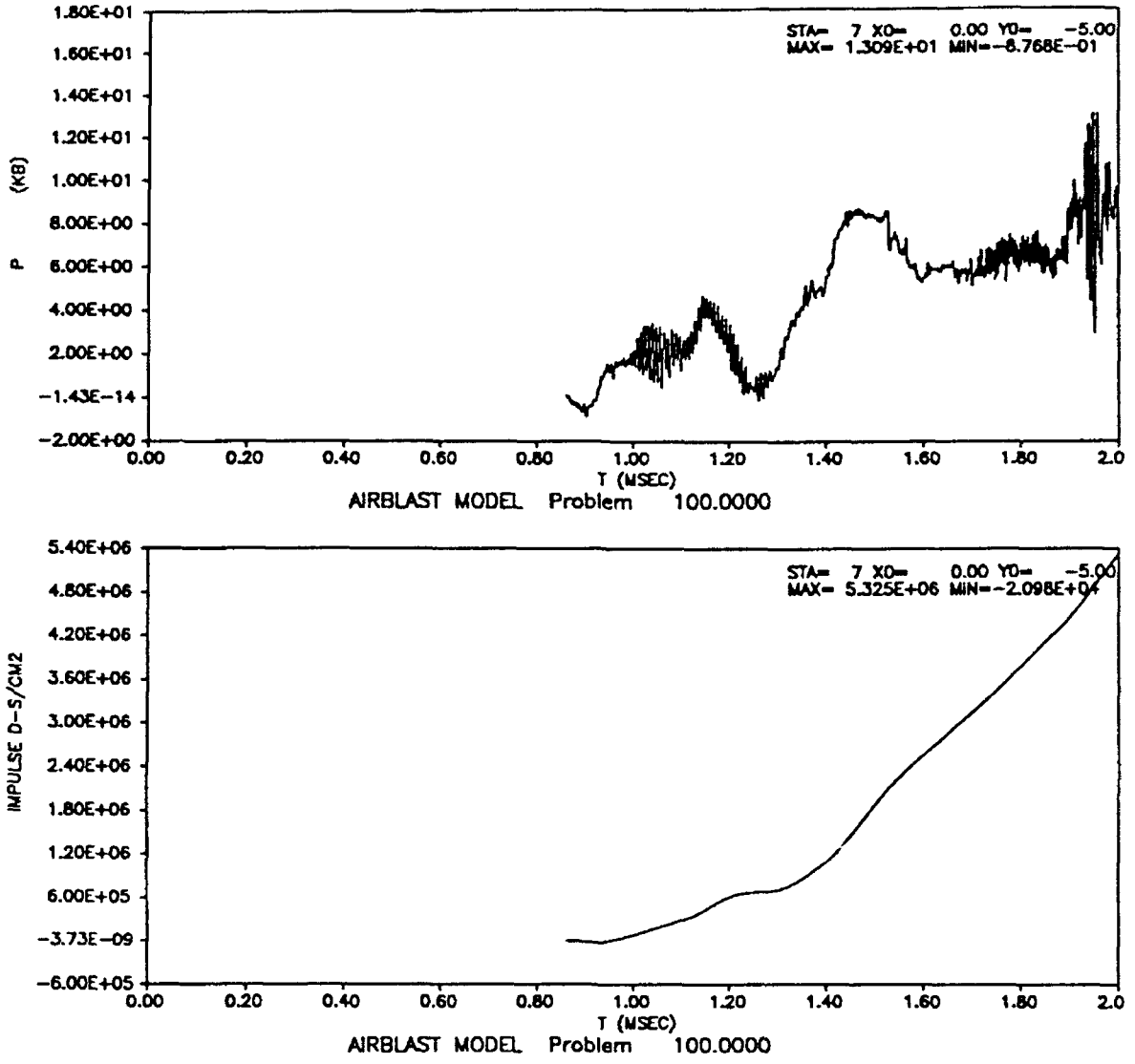

Figure 26. Pressure time history at 5.0 cm below ground zero, near center of steel cylinder.

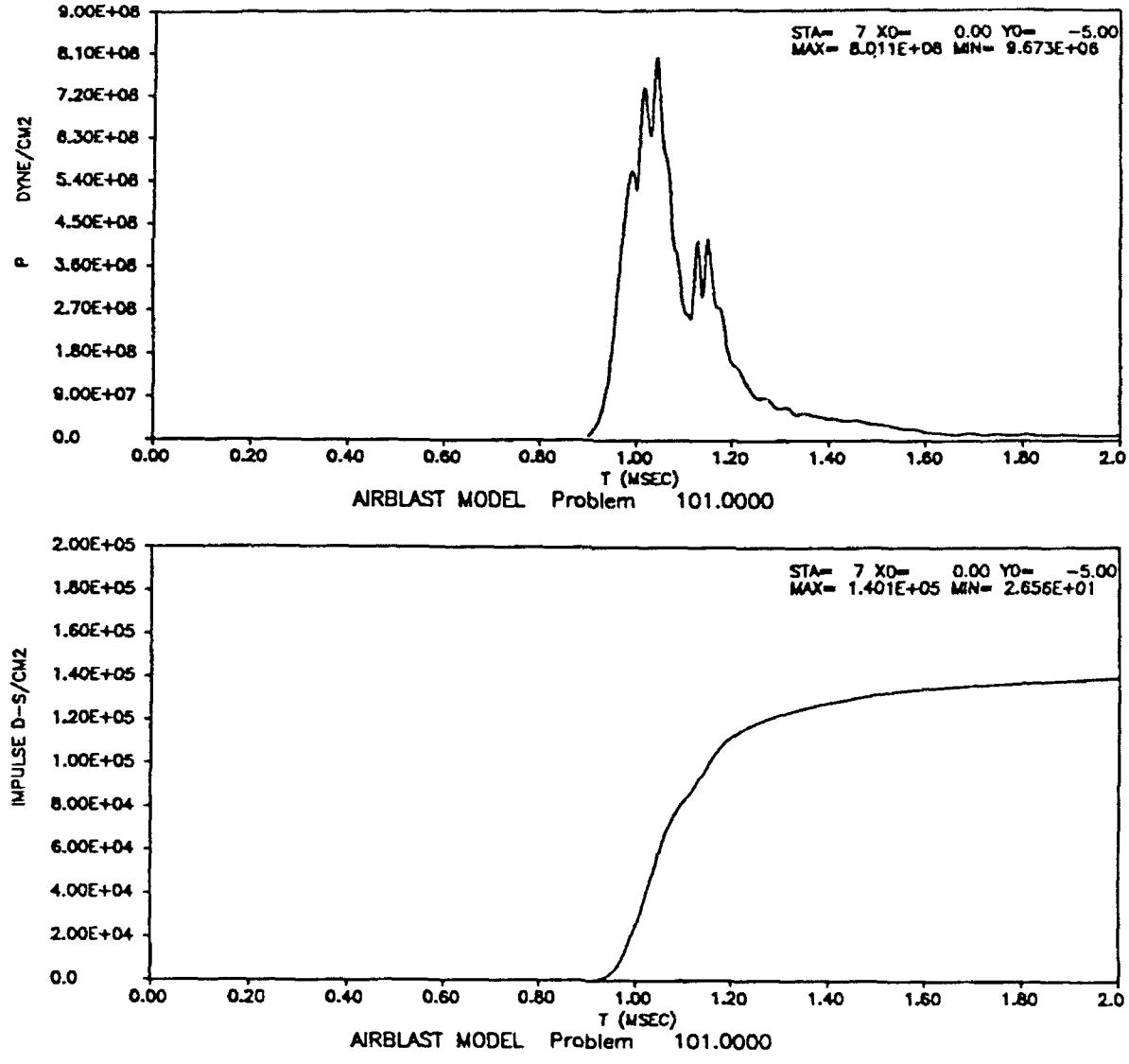

Figure 27. Pressure time history at 5.0 cm below ground zero, with no gage mount.

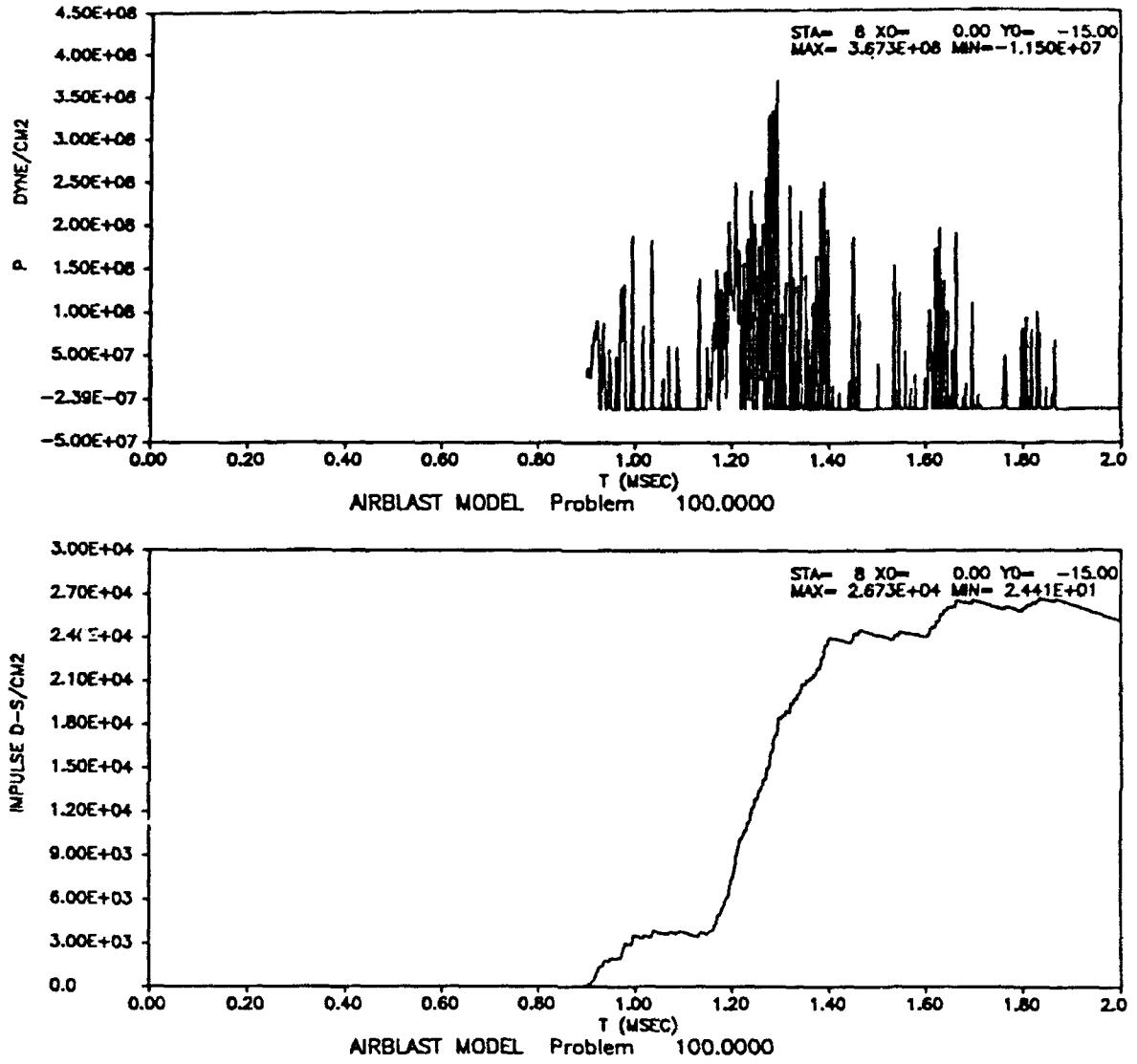

Figure 28. Pressure time history at 15.0 cm below ground zero, in concrete housing below steel cylinder.

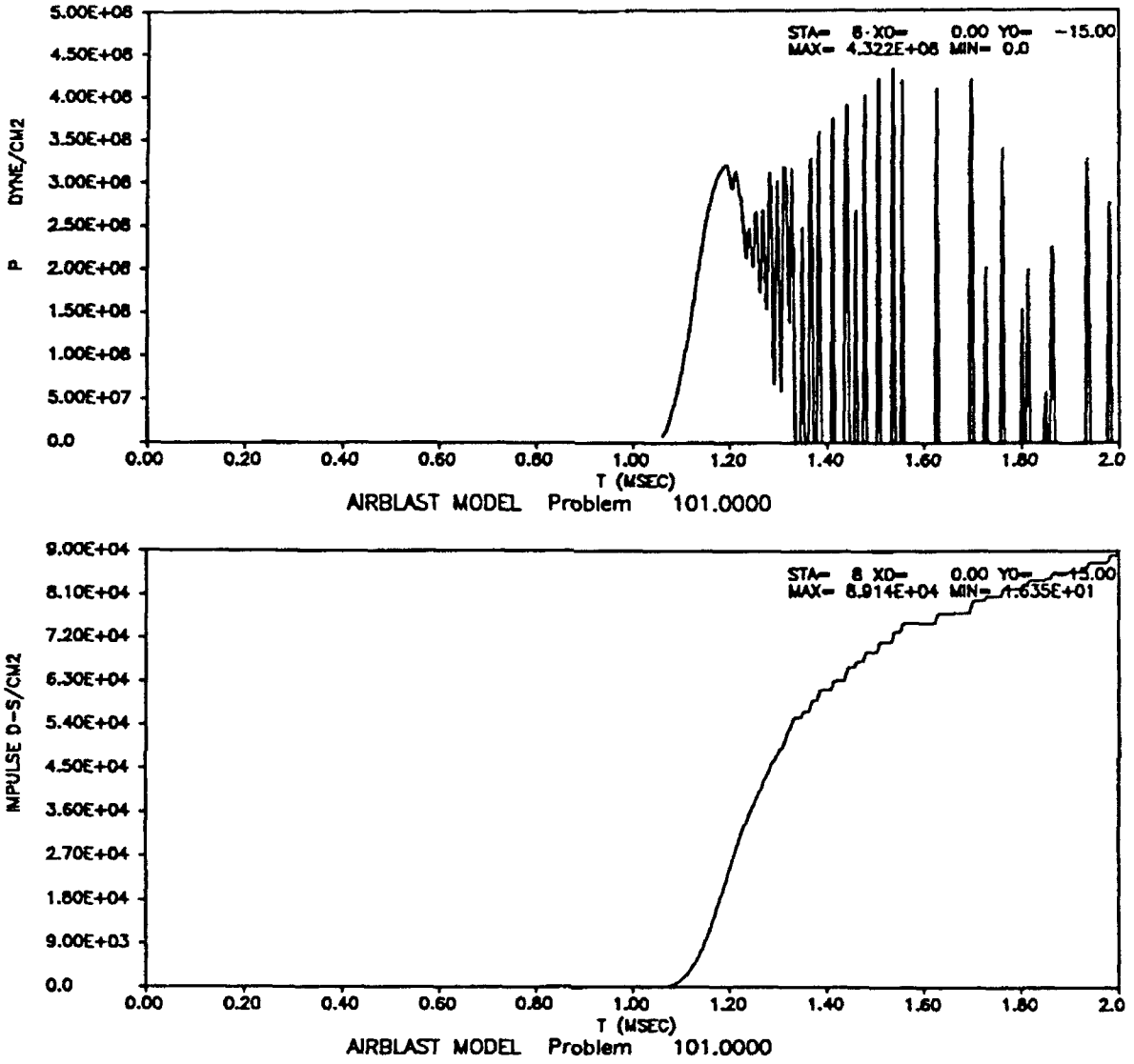

Figure 29. Pressure time history at 15.0 cm below ground zero, with no gage mount.

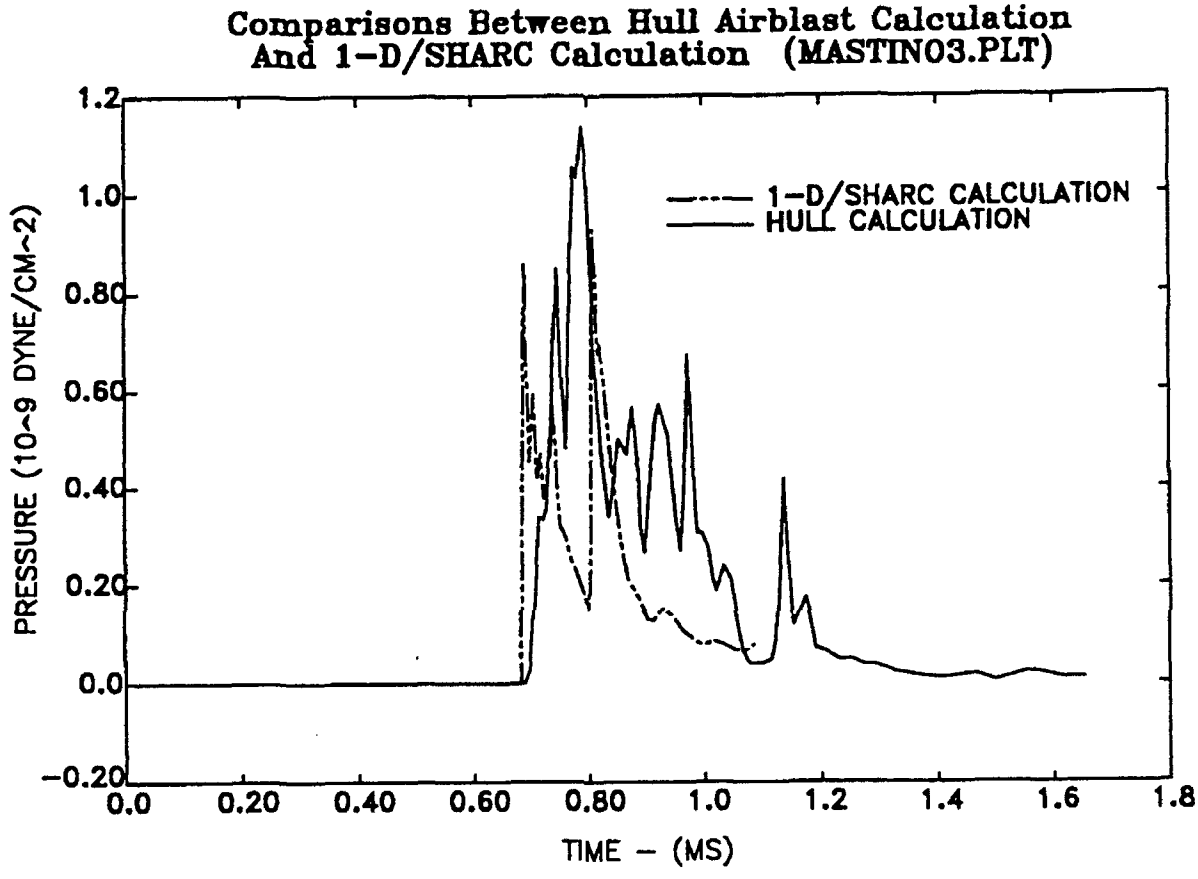

Figure 30. Comparison of HULL-calculated pressure time history at ground zero with results from a SHARC calculation. The HULL solution has been shifted to match the experimental time-of-arrival.

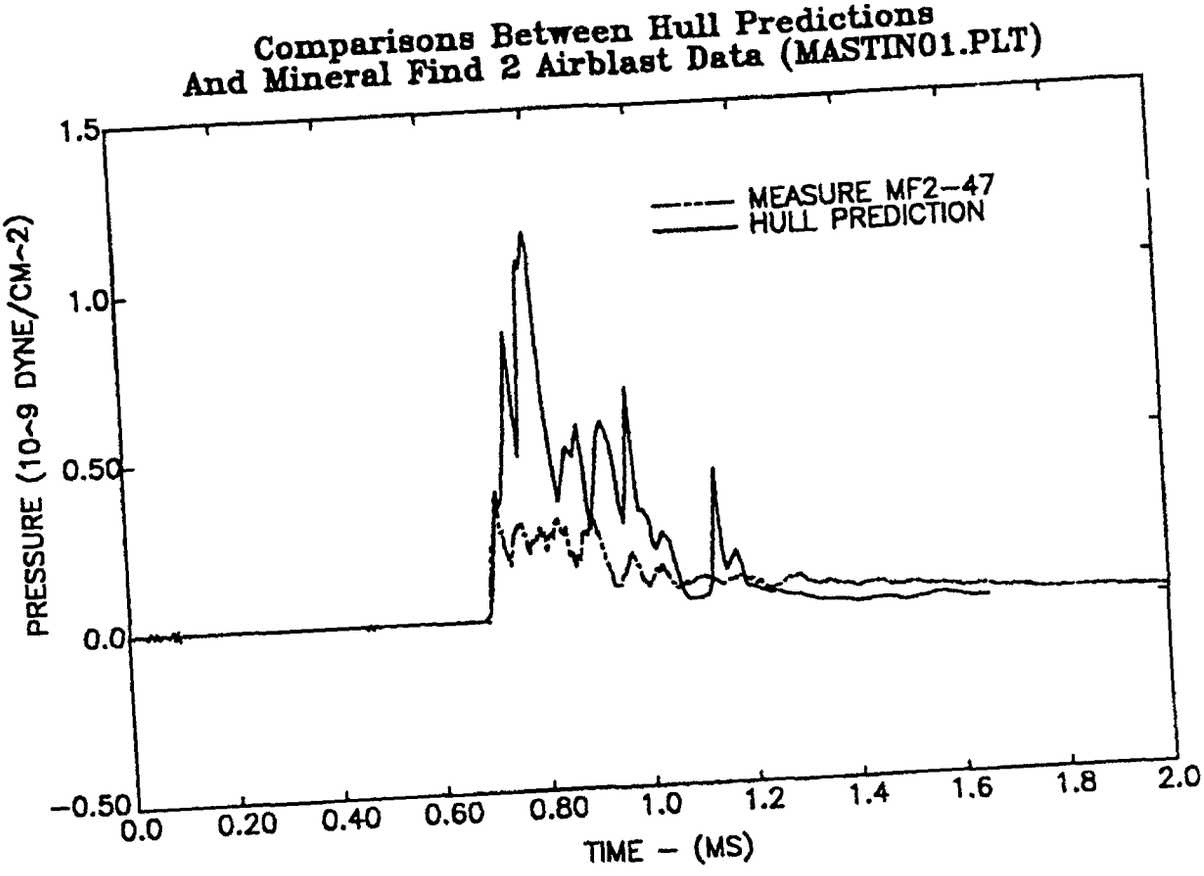

Figure 31. Comparison of HULL-calculated pressure time history at ground zero with results from the Mineral Find II, gage no. 47. The HULL solution has been shifted to match the experimental time-of-arrival.

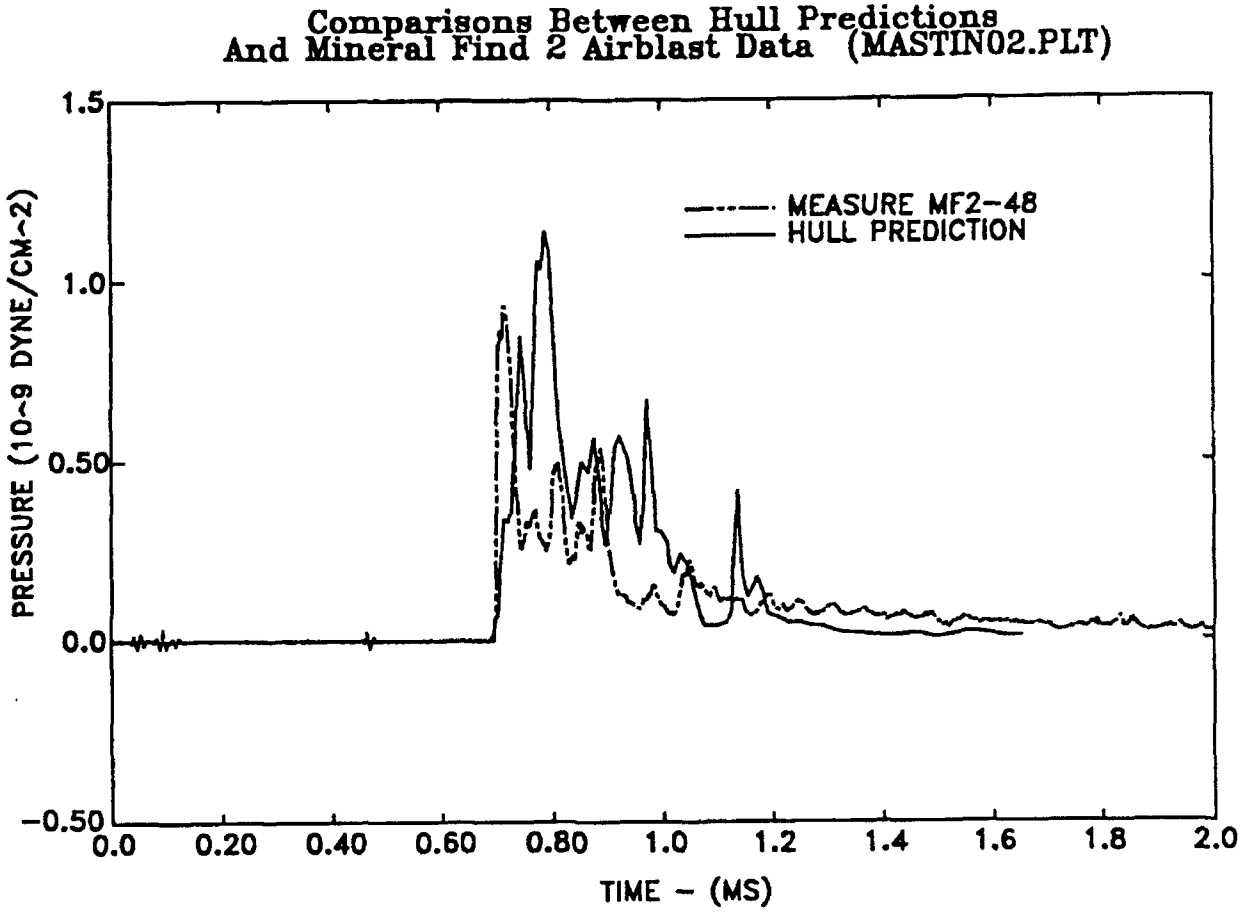

Figure 32. Comparison of HULL-calculated pressure time history at ground zero with results from the Mineral Find II, gage no. 48. The HULL solution has been shifted to match the experimental time-of-arrival.

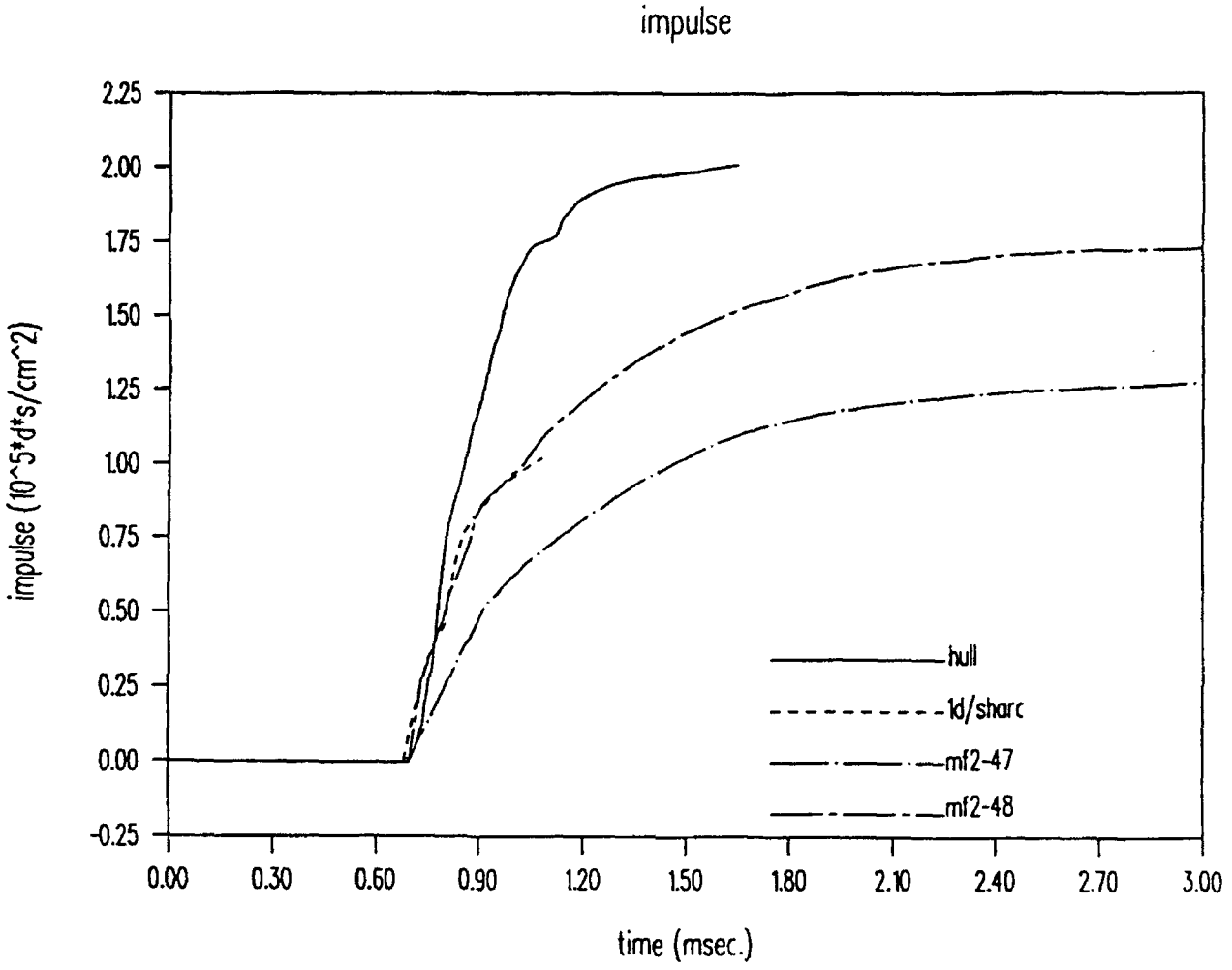

Figure 33. Pressure impulse time history at ground zero from HULL and SHARC calculations compared with results of the Mineral Find II experiment. The HULL solution has been shifted to match the experimental time-of-arrival.

REPORT DOCUMENTATION PAGE

Form Approved
OMB No. 0704-0188

1. AGENCY USE ONLY (Leave blank)	2. REPORT DATE	3. REPORT TYPE AND DATES COVERED
	July 1993	Final Report

4. TITLE AND SUBTITLE
Simulation of Gage-Mount Responses in Airblast tests

5. FUNDING NUMBERS
Contract No.:
DACA39-90-M-3694

6. AUTHOR(S)
C. Wayne Mastin

7. PERFORMING ORGANIZATION NAME(S) AND ADDRESS(ES)
Department of Mathematics and Statistics
Mississippi State University
Mississippi State, Mississippi 39762

8. PERFORMING ORGANIZATION REPORT NUMBER

9. SPONSORING/MONITORING AGENCY NAME(S) AND ADDRESS(ES)
Defense Nuclear Agency
Kirtland Air Force Base, New Mexico 87117-5000
U.S. Army Engineer Waterways Experiment Station
Structures Laboratory, 3909 Halls Ferry Road,
Vicksburg, Mississippi 39180-6199

10. SPONSORING/MONITORING AGENCY REPORT NUMBER
Miscellaneous Paper
SL-93-8

11. SUPPLEMENTARY NOTES
Available from National Technical Information Service,
5285 Port Royal Road, Springfield, VA 22161

12a. DISTRIBUTION/AVAILABILITY STATEMENT
Approved for public release, distribution limited

12b. DISTRIBUTION CODE

13. ABSTRACT (Maximum 200 words)

The HULL hydrodynamics code was used to simulate the Mineral Find II event. Computed pressure and impulse values were within the uncertainty interval of the experimental data. The numerical solution exhibits oscillations at the gage which are approximately the same frequency as the experimental data. The numerical solution also developed numerical instabilities and excessive dissipation which are due to the algorithm used in the HULL code. Except for the prediction of a longer arrival time, the computational results give a good qualitative simulation of the experiment. In order to determine the gage-mount response, a similar problem without the gage mount is also solved.

14. SUBJECT TERMS
Airblast, Gage mount, Hydrocode

15. NUMBER OF PAGES
45

16. PRICE CODE

17. SECURITY CLASSIFICATION OF REPORT	18. SECURITY CLASSIFICATION OF THIS PAGE	19. SECURITY CLASSIFICATION OF ABSTRACT	20. LIMITATION OF ABSTRACT
UNCLASSIFIED	UNCLASSIFIED	UNCLASSIFIED	

Destroy this report when no longer needed. Do not return it to the originator.